1. Supplementary Tables

Supplementary Table 1: DAKD and its analogues used in this work with different isotope labeling schemes or chemical modifications. Peptides for ssNMR experiments were uniformly ^{13}C,^{15}N-labelled on specific residue sites.

Peptide	Labeling scheme	Abbreviation
DAKD	(^{13}C,^{15}N)K-RPPGFSPF (a)	U-[^{13}C,^{15}N]-K_1 DAKD
	K-(^{13}C,^{15}N)R-PPGF-(^{13}C,^{15}N)S-PF (b)	U-[^{13}C,^{15}N]-R_2S_7 DAKD
	KR-(^{13}C,^{15}N)P-PGFSPF (a)	U-[^{13}C,^{15}N]-P_3 DAKD
	KRP-(^{13}C,^{15}N)P-GFSPF (a)	U-[^{13}C,^{15}N]-P_4 DAKD
	KRPP-(^{13}C,^{15}N)G-(^{13}C,^{15}N)F-SPF (a)	U-[^{13}C,^{15}N]-G_5F_6 DAKD
	KRPPGFS-(^{13}C,^{15}N)P-(^{13}C,^{15}N)F (b)	U-[^{13}C,^{15}N]-S_7P_8 DAKD
DALK	KRPPGFS-(^{13}C,^{15}N)P-(^{13}C,^{15}N)L (a)	U-[^{13}C,^{15}N]-P_8L_9 DALK
DAKD(N-Methyl F6)	KRPPG-(N-Methyl)F-SPF (a)	DAKD(N-Methyl F6)

(a) Thermo Fisher Scientific, Ulm, Germany, (b) Eurogentec, Cologne, Germany

Supplementary Table 2: Chemical Shift assignment of DAKD bound to B_1R*

Residue	Atoms								
	N	C'	Cα	Cβ	Cγ	Cδ	Cε	Cζ	N(sidechain)
K1	40.2	173.8	55.9	33.4	-	29.5	41.8		32.5 (Nζ)
R2	121.5	174.8	55.0	30.8	27.5	43.3		158.7	83.5 (Nε) 73.6(Nη)
P3	133.9	175.7	61.7	31.2	28.5	50.6			
P4	131.7	177.4	63.5	32.5	28.4	50.4			
G5	111.9	174.7	45.2						
F6	118.7	178.5	59.0	40.1	129.1	131.7	131.7	134.1	
S7	121.8	174.4	55.4	62.6					
P8	135.1	175.9	62.7	32.7	28.5	50.6			
F9	124.4	181.0	57.3	39.4	128.5	131.6	131.6	133.8	

* ^{13}C chemical shifts (in ppm) are referenced to TSP.
* ^{15}N chemical shifts (in ppm) are referenced to liquid NH_3.

Supplementary Table 3: Chemical Shift assignment of DAKD without B_1R* (solid-state NMR)

Residue	Atoms							
	N	C'	Cα	Cβ	Cγ	Cδ	Cε	Cζ	N(sidechain)
K1	40.7	173.4	55.5	33.6	22.5	29.4	42.2		33.4 (Nζ)
R2	121.1	175.1	55.0	30.3	26.8	43.2		158.8	83.2 (Nε) 72.6(Nη)
P3	133.2	174.8	61.8	31.1	27.9	50.8			
P4	130.7	178.3	63.3	32.7	28.3	50.6			
G5	111.3	174.7	45.1						
F6	118.5	178.6	58.7	40.0	129.3	132.2	132.2	134.7	
S7	121.1	174.0	56.1	62.7					
P8	135.8	176.0	62.6	32.8	28.5	51.0			
F9	126.5	181.6	58.6	39.8	129.1	130.8	132.3	132.9	

* ^{13}C chemical shifts (in ppm) are referenced to TSP.
* ^{15}N chemical shifts (in ppm) are referenced to liquid NH_3.

Supplementary Table 4: Chemical Shift Differences of bound DAKD – free DAKD (solid-state NMR)

Residue	Atoms								
	N	C'	Cα	Cβ	Cγ	Cδ	Cε	Cζ	N(sidechain)
K1	-0.5	+0.4	+0.4	-0.2		+0.1	-0.4		-0.9 (Nζ)
R2	+0.4	-0.3	0.0	+0.5	+0.7	+0.1		-0.1	+0.3(Nε) +1.0(Nη)
P3	+0.7	+0.9	-0.1	+0.1	+0.6	-0.2			
P4	+1.0	-0.9	+0.2	-0.2	+0.1	-0.2			
G5	+0.6	0.0	+0.1						
F6	+0.2	-0.1	+0.3	+0.1	-0.2	-0.5	-0.5	-0.6	
S7	+0.7	+0.4	-0.7	-0.1					
P8	-0.7	-0.1	+0.1	-0.1	0.0	-0.4			
F9	-2.1	-0.6	-1.3	-0.4	-0.6	+0.8	-0.7	+0.9	

* ^{13}C chemical shifts (in ppm) are referenced to TSP.
* ^{15}N chemical shifts (in ppm) are referenced to liquid NH_3.

Supplementary Table 5: Chemical Shift assignment of DAKD without B$_1$R* in solution without detergent at 298K *

298K, H2O/D2O, 50mM MES, pH5.6, 100mM NaCl

Residue	Atoms												
	N	NH	C’	Cα	Cβ	Cγ	Cδ	Cε	Hα	Hβ	Hγ	Hδ	Hε
K1	-	-	172.3	55.5	33.2	23.8	29.1	41.9	3.94	1.79	1.34	1.60	2.90
R2	125.1	8.66	173.3	54.2	30.0	26.7	43.3		4.50	1.62	1.54	2.98	7.01
P3	-		174.4	-	30.7	27.3	50.6		-	1.79/2.28	1.92	2.74/3.39	
P4	-		177.4	63.3	31.9	27.4	50.4		4.30	1.80/2.19	1.94	3.56/3.71	
G5	109.1	8.35	173.7	45.0					3.74/3.83				
F6	120.2	7.89	175.3	57.9	39.8	-	-	-	4.45	2.94	-	7.11	7.22
S7	119.8	8.04	172.3	55.5	63.7				4.54	3.61			
P8	-		175.3	63.4	31.7	26.7	50.6		4.20	1.71/2.04	1.60/1.80	3.46	
F9	123.5	7.33	180.0	58.7	40.2	-	-	-	4.32	2.84/3.04	-	7.13	7.24

* ^{13}C chemical shifts (in ppm) are referenced to TSP.

* ^{15}N chemical shifts (in ppm) are referenced to liquid NH$_3$.

Supplementary Table 6: Solution NMR and refinement statistics for free DAKD in solution without detergents

	ARIA	CYANA (TALOS+)	CYANA (TALOS-N)	Forward cluster A
NMR distance and dihedral constraints				
Distance constraints				
Total NOE	73	-	-	-
Intra-residue	48	-	-	-
Inter-residue				
Sequential (|*i* – *j*| = 1)	24	-	-	-
Medium-range (|*i* – *j*| < 4)	1	-	-	-
Long-range (|*i* – *j*| > 5)	-	-	-	-
Intermolecular	-	-	-	-
Hydrogen bonds	0	-	-	-
Total dihedral angle restraints	14	11	11	11
ϕ	7	4	4	4
ψ	7	7	7	7
Structure statistics				
Violations (mean and s.d.)				
Distance constraints (Å)	0.039 ± 0.002	-	-	-
Dihedral angle constraints (º)	0.83 ± 0.19	2.64 ± 0.88	2.56 ± 0.87	0.20 ± 0.07
Max. dihedral angle violation (º)	5.42	11.90	15.35	2.22
Max. distance constraint violation (Å)	0.312	-	-	-
Number of CYANA restraints violations*	-	3	2	0
CYANA target function (10^{-2})	-	1.59	1.88	0.75
Deviations from idealized geometry				
Bond lengths (Å)	0.008	0.001	0.001	0.001
Bond angles (º)	0.6	0.3	0.3	0.3
Impropers (º)	1.05	0.64	0.64	0.64
Average pairwise r.m.s. deviation** (Å)				
Heavy	2.80 ± 0.73 (20)	1.63 ± 0.24 (10)	1.57 ± 0.23 (10)	1.68 ± 0.24 (10)
Backbone	1.29 ± 0.47 (20)	0.57 ± 0.13 (10)	0.53 ± 0.12 (10)	0.58 ± 0.13 (10)
Ramachandran distribution				
Most favored (%)	98.3	100	100	100
Additional allowed (%)	1.7	0	0	0
Generally allowed (%)	0	0	0	0
Disallowed region (%)	0	0	0	0

* Violations are counted if at least 3 out of 10 structural models show violation

** The number of structural models for computing pairwise r.m.s. deviation was listed in ( ).

Supplementary Table 7: ssNMR and refinement statistics for DAKD bound to B1R

	CYANA (TALOS+)	**CYANA (TALOS-N)**	**CYANA (PREDITOR)**	**Forward cluster A**
NMR distance and dihedral constraints				
Distance constraints				
Total NOE	-	-	-	-
Intra-residue	-	-	-	-
Inter-residue				
Sequential ($\|i - j\| = 1$)	-	-	-	-
Medium-range ($\|i - j\| < 4$)	-	-	-	-
Long-range ($\|i - j\| > 5$)	-	-	-	-
Intermolecular	-	-	-	-
Hydrogen bonds	-	-	-	-
Total dihedral angle restraints	11	11	10	13
ϕ	4	4	4	5
ψ	7	7	6	8
Structure statistics				
Violations (mean and s.d.)				
Distance constraints (Å)	-	-	-	-
Dihedral angle constraints (º)	0.43 ± 0.14	1.00 ± 0.43	0.87 ± 0.29	0.78 ± 0.26
Max. dihedral angle violation (º)	4.78	10.85	8.72	5.48
Max. distance constraint violation (Å)	-	-	-	-
Number of CYANA restraints violations*	0	2	2	1
CYANA target function (10^{-3})	7.61	14.7	7.11	8.53
Deviations from idealized geometry				
Bond lengths (Å)	0.001	0.001	0.001	0.001
Bond angles (º)	0.3	0.3	0.3	0.3
Impropers (º)	0.64	0.64	0.64	0.64
Average pairwise r.m.s. deviation** (Å)				
Heavy	1.67 ± 0.18	1.46 ± 0.31	2.07 ± 0.31	1.49 ± 0.34
Backbone	0.50 ± 0.09	0.36 ± 0.10	0.82 ± 0.23	0.39 ± 0.12
Ramachandran distribution				
Most favored (%)	100	97	60	100
Additional allowed (%)	0	3	40	0
Generally allowed (%)	0	0	0	0
Disallowed region (%)	0	0	0	0

* Violations are counted if at least 3 out of 10 structural models show violation

** Pairwise r.m.s. deviations were calculated on 10 structural models.

Supplementary Table 8: SSNMR and TALOS+/CYANA refinement statistics for DAKD and BK in different states

	DAKD (+ B1R)	DAKD (- B1R)	BK (+ B2R)	BK (- B2R)
NMR distance and dihedral constraints				
Distance constraints				
Total NOE	-	-	-	-
Intra-residue	-	-	-	-
Inter-residue				
Sequential ($\|i - j\| = 1$)	-	-	-	-
Medium-range ($\|i - j\| < 4$)	-	-	-	-
Long-range ($\|i - j\| > 5$)	-	-	-	-
Intermolecular	-	-	-	-
Hydrogen bonds	-	-	-	-
Total dihedral angle restraints	11	11	10	10
ϕ	4	4	4	4
ψ	7	7	6	6
Structure statistics				
Violations (mean and s.d.)				
Distance constraints (Å)	-	-	-	-
Dihedral angle constraints (º)	0.43 ± 0.14	1.99 ± 0.67	2.32 ± 0.77	0.64 ± 0.21
Max. dihedral angle violation (º)	4.78	10.59	23.21	6.36
Max. distance constraint violation (Å)	-	-	-	-
Number of CYANA restraints violations*	0	2	1	1
CYANA target function (10^{-3})	7.61	13.8	21.1	5.07
Deviations from idealized geometry				
Bond lengths (Å)	0.001	0.001	0.001	0.001
Bond angles (º)	0.3	0.3	0.3	0.3
Impropers (º)	0.64	0.65	0.62	0.63
Average pairwise r.m.s. deviation** (Å)				
Heavy	1.67 ± 0.18	1.73 ± 0.25	1.63 ± 0.22	2.29 ± 0.42
Backbone	0.50 ± 0.09	0.43 ± 0.12	0.28 ± 0.07	0.58 ± 0.12
Ramachandran distribution				
Most favored (%)	100	100	77	97
Additional allowed (%)	0	0	23	3
Generally allowed (%)	0	0	0	0
Disallowed region (%)	0	0	0	0

* Violations are counted if at least 3 out of 10 structural models show violation

** Pairwise r.m.s. deviations were calculated on 10 structural models.

Supplementary Table 9: Summary of GPCR template X-ray structures used for B_1R/B_2R comparative modeling.

Template Name	Species	Sequence identity to B_1R (%)	Sequence identity to B_2R (%)	PDB code	Resolution (Å)	Reference
angiotensin II type 1 receptor	human	33	34	4yay	2.9	1
C-C chemokine receptor type 5	human	28	24	4mbs	2.7	2
κ-opioid receptor	human	24	27	4djh	2.9	3
orexin receptor type 2	human	20	21	4s0v	2.5	4
P_2Y_1 receptor	human	22	25	4xnv	2.2	5
δ-opioid receptor	human	26	26	4n6h	1.8	6
μ-opioid receptor	human	24	26	4dkl	2.8	7
lysophosphatidic acid receptor 1	human	21	18	4z35	2.9	8
nociceptin receptor	human	24	27	4ea3	3.0	9
rhodopsin	bovine	21	23	2x72	3.0	10
5-hydroxytryptamine receptor 2B	human	19	21	4ib4	2.7	11
β_1-adrenergic receptor	turkey	19	19	2y03	2.9	12
proteinase-activated receptor 1	human	20	24	3vw7	2.2	13
muscarinic acetylcholine receptor M2	human	19	20	3uon	3.0	14
histamine H1 receptor	human	22	21	3rze	3.1	15
muscarinic acetylcholine receptor M3	rat	18	21	4u15	2.8	16
β_2-adrenergic receptor	human	19	20	3sn6	3.2	17
β_2-adrenergic receptor	human	19	21	2rh1	2.4	18
adenosine receptor A2a	human	21	22	3qak	2.7	19
adenosine receptor A2a	human	21	22	3eml	2.6	20
sphingosine 1-phosphate receptor 1	human	21	21	3v2y	2.8	21
dopamine D3 receptor	human	20	25	3pbl	2.9	22
5-hydroxytryptamine receptor 1B	human	19	21	4iar	2.7	23
free fatty acid receptor 1	human	19	15	4phu	2.3	24

Supplementary Table 10: Multiple sequence alignment between 24 GPCR templates and the B_1R and B_2R sequence which was used for comparative modeling with Rosetta. Highly conserved residues are highlighted in orange boxes. Helix and β-sheet regions as observed in the crystal structure of the GPCR templates or predicted by PSIPRED and OCTOPUS for B_1R and B_2R are colored green and blue, respectively.

PDB ID	
2x72	NFYVPFSNKTGVVRSPFEAPQYYLAEPWQFSMLAAYMFLLIMLGFPINFLTLYVTVQHKKLR
2rh1	-------------------------DEVWVVGMGIVMSLIVLAIVFGNVLVITAIAKFERLQ
3sn6	--------------------------EVWVVGMGIVMSLIVLAIVFGNVLVITAIAKFERLQ
2y03	---------------------AELLSQQWEAGMSLLMALVVLLIVAGNVLVIAAIGSTQRLQ
3eml	--------------------------IMGSSVYITVELAIAVLAILGNVLVCWAVWLNSNLQ
3qak	--------------------------IMGSSVYITVELAIAVLAILGNVLVCWAVWLNSNLQ
4ib4	-----------------------EEQGNKLHWAALLILMVIIPTIGGNTLVILAVSLEKKLQ
4iar	------------------YIYQDSISLPWKVLLVMLLALITLATTLSNAFVIATVYRTRKLH
4u15	-------------------------TIWQVVFIAFLTGFLALVTIIGNILVIVAFKVNKQLK
3rze	------------------------------MPLVVVLSTICLVTVGLNLLVLYAVRSERKLH
3v2y	VSDYVNYDIIVRHYNYTGKLNISADKENSIKLTSVVFILICCFIILENIFVLLTIWKTKKFH
4djh	-------------------------SPAIPVIITAVYSVVFVVGLVGNSLVMFVIIRYTKMK
4ea3	-------------------------PLGLKVTIVGLYLAVCVGGLLGNCLVMYVILRHTKMK
3pbl	--------------------------------YALSYCALILAIVFGNGLVCMAVLKERALQ
3uon	--------------------------TFEVVFIVLVAGSLSLVTIIGNILVMVSIKVNRHLQ
4z35	---QCFYNESIAFFYNRSGKHLATEWNTVSKLVMGLGITVCIFIMLANLLVMVAIYVNRRFH
4dkl	--------------------------MVTAITIMALYSIVCVVGLFGNFLVMYVIVRYTKMK
4n6h	----------------GSPGARSASSLALAIAITALYSAVCAVGLLGNVLVMFGIVRYTKMK
4yay	-------------ILNSSDCPKAGRHNYIFVMIPTLYSIIFVVGIFGNSLVVIVIYFYMKLK
4xnv	-----------------SFKCALTKTGFQFYYLPAVYILVFIIGFLGNSVAIWMFVFHMKPW
4mbs	------------------PCQKINVKQIAARLLPPLYSLVFIFGFVGNMLVILILINYKRLK
4s0v	-------------------------PKEYEWVLIAGYIIVFVVALIGNVLVCVAVWKNHHMR
4phu	-------------------------MDLPPQLSFGLYVAAFALGFPLNVLAIRGATAHARLR
3vw7	------------------DASGYLTSSWLTLFVPSVYTGVFVVSLPLNIMAIVVFILKMKVK
b1_r	------------------------AWDLLHRVLPTFIISICFFGLLGNLFVLLVFLLPRRQL
b2_r	----------------------VEWLGWLNTIQPPFLWVLFVLATLENIFVLSVFCLHKSSC

PDB ID	
2x72	-TPLNYILLNLAVADLFMVFGGFTTTLYTSLHG-YFVFGPTGCNLQGFFATLGGEIALWSLV
2rh1	-TVTNYFITSLACADLVMGLAVVPFGAAHILMK-MWTFGNFWCEFWTSIDVLCVTASIETLC
3sn6	-TVTNYFITSLACADLVMGLAVVPFGAAHILTK-TWTFGNFWCEFWTSIDVLCVTASIETLC
2y03	-TLTNLFITSLACADLVVGLLVVPFGATLVVRG-TWLWGSFLCELWTSLDVLCVTASIETLC
3eml	-NVTNYFVVSLAAADIAVGVLAIPFAITISTG---FCAACHGCLFIACFVLVLTQSSIFSLL
3qak	-NVTNYFVVSLAAADIAVGVLAIPFAITISTG---FCAACHGCLFIACFVLVLTQSSIFSLL
4ib4	-YATNYFLMSLAVADLLVGLFVMPIALLTIMFEAMWPLPLVLCPAWLFLDVLFSTASIWHLC
4iar	-TPANYLIASLAVTDLLVSILVMPISTMYTVTG-RWTLGQVVCDFWLSSDITCCTASIWHLC
4u15	-TVNNYFLLSLACADLIIGVISMNLFTTYIIMN-RWALGNLACDLWLSIDYVASNASVMNLL
3rze	-TVGNLYIVSLSVADLIVGAVVMPMNILYLLMS-KWSLGRPLCLFWLSMDYVASTASIFSVF
3v2y	-RPMYYFIGNLALSDLLAGV-AYTANLLLSGAT-TYKLTPAQWFLREGSMFVALSASVFSLL
4djh	-TATNIYIFNLALADALVTT-TMPFQSTVYLMN-SWPFGDVLCKIVLSIDYYNMFTSIFTLT
4ea3	-TATNIYIFNLALADTLVLL-TLPFQGTDILLG-FWPFGNALCKTVIAIDYYNMFTSTFTLT
3pbl	-TTTNYLVVSLAVADLLVATLVMPWVVYLEVTGGVWNFSRICCDVFVTLDVMMCTASIWNLC
3uon	-TVNNYFLFSLACADLIIGVFSMNLYTLYTVIG-YWPLGPVVCDLWLALDYVVSNASVMNLL
4z35	-FPIYYLMANLAAADFFAGL-AYFYLMFNTGPN-TRRLTVSTWLLRQGLIDTSLTASVANLL
4dkl	-TATNIYIFNLALADALATS-TLPFQSVNYLMG-TWPFGNILCKIVISIDYYNMFTSIFTLC
4n6h	-TATNIYIFNLALADALATS-TLPFQSAKYLME-TWPFGELLCKAVLSIDYYNMFTSIFTLT
4yay	-TVASVFLLNLALADLCFLL-TLPLWAVYTAMEYRWPFGNYLCKIASASVSFNLYASVFLLT
4xnv	-SGISVYMFNLALADFLYVL-TLPALIFYYFNKTDWIFGDAMCKLQRFIFHVNLYGSILFLT
4mbs	-SMTDIYLLNLAISDLFFLL-TVPFWAHYAAA--QWDFGNTMCQLLTGLYFIGFFSGIFFII
4s0v	-TVTNYFIVNLSLADVLVTITCLPATLVVDITE-TWFFGQSLCKVIPYLQTVSVSVSVLTLS
4phu	LTPSAVYALNLGCSDLLLTV-SLPLKAVEALASGAWPLPASLCPVFAVAHFAPLYAGGGFLA
3vw7	-KPAVVYMLHLATADVLFVS-VLPFKISYYFSGSDWQFGSELCRFVTAAFYCNMYASILLMT
b1_r	-NVAEIYLANLAASDLVFVL-GLPFWAENIWNQFNWPFGALLCRVINGVIKANLFISIFLVV
b2_r	-TVAEIYLGNLAAADLILAC-GLPFWAITISNNFDWLFGETLCRVVNAIISMNLYSSICFLM

PDB ID	
2x72	VLAIERYVVVCKPMSN----FRFGENHAIMGVAFTWVMALACAA-PPLVGWS-----R----
2rh1	VIAVDRYFAITSPFKYQ---SLLTKNKARVIILMVWIVSGLTSFLPIQMHWY----------
3sn6	VIAVDRYFAITSPFKYQ---SLLTKNKARVIILMVWIVSGLTSFLPIQMHWY----------
2y03	VIAIDRYLAITSPFRYQ---SLMTRARAKVIICTVWAISALVSFLPIMMHWW----------
3eml	AIAIDRYIAIRIPLRYN---GLVTGTRAKGIIAICWVLSFAIGL-TPMLGWN----------
3qak	AIAIDRYIAIRIPLRYN---GLVTGTRAKGIIAICWVLSFAIGL-TPMLGWN----------
4ib4	AISVDRYIAIKKPIQAN---QYNSRATAFIKITVVWLISIGIAIPVPIK-------------
4iar	VIALDRYWAITDAVEYS---AKRTPKRAAVMIALVWVFSISISLPPF--FW-----------
4u15	VISFDRYFSITRPLTYR---AKRTTKRAGVMIGLAWVISFVLWAPAILF-WQYFVGKR----
3rze	ILCIDRYRSVQQPLRYL---KYRTKTRASATILGAWFLSFLWVIP-ILG-WNH---------
3v2y	AIAIERYITMLK-----------NNFRLFLLISACWVISLILGG-LPIMGWN----------
4djh	MMSVDRYIAVCHPVKAL---DFRTPLKAKIINICIWLLSSSVGISAIVLG------------
4ea3	AMSVDRYVAICHP----------TSSKAQAVNVAIWALASVVGVPVAIMG------------
3pbl	AISIDRYTAVVMPVHYQHGTGQSSCRRVALMITAVWVLAFAVSC-PLLFGFN----------
3uon	IISFDRYFCVTKPLTYP---VKRTTKMAGMMIAAAWVLSFILWAPAILF-WQFIVGVR----
4z35	AIAIERHITVFRMQLH----TRMSNRRVVVVIVVIWTMAIVMGA-IPSVGWN----------
4dkl	TMSVDRYIAVCHPVKAL---DFRTPRNAKIVNVCNWILSSAIGLPVMFMA------------
4n6h	MMSVDRYIAVCHPVKAL---DFRTPAKAKLINICIWVLASGVGVPIMVMA------------
4yay	CLSIDRYLAIVHPMKSR---LRRTMLVAKVTCIIIWLLAGLASLPAIIHR------------
4xnv	CISAHRYSGVVYP-KSL---GRLKKKNAICISVLVWLIVVVAISPILFYS------------
4mbs	LLTIDRYLAVVHAVFAL---KARTVTFGVVTSVITWVVAVFASLPNIIFT------------
4s0v	CIALDRWYAICHP---------STAKRARNSIVIIWIVSCIIMIPQAIVM------------
4phu	ALSAARYLGAAFP-----------PCYSWGVCAAIWALVLCHLGLVFGLEA-PGGWLDHSNT
3vw7	VISIDRFLAVVYPM--------RTLGRASFTCLAIWALAIAGVV-PLLLKE-----------
b1_r	AISQDRYRVLVHPMASR---RQQRRRQARVTCVLIWVVGGLLSIPTFLLR------------
b2_r	LVSIDRYLALVKTMSMG---RMRGVRWAKLYSLVIWGCTLLLSSPMLVFR------------

PDB ID	
2x72	--------YIP------E-GM-----QCSCGIDY-YTPHEETNNESFVIYMFVVHFIIPLIV
2rh1	--R-----ATHQEAINCY-AE-----ETCCDFF---------TNQAYAIASSIVSFYVPLVI
3sn6	--R--------QEAINCY-AE-----ETCCDFF---------TNQAYAIASSIVSFYVPLVI
2y03	--R-----DEDPQALKCY-QD-----PGCCDFV---------TNRAYAIASSIISFYIPLLI
3eml	--NCGQSQG----------CG---EGQVACLFED------VVPMNYMVYFNFFACVLVPLLL
3qak	--NCGQ--G----------CG---EGQVACLFED------VVPMNYMVYFNFFACVLVPLLL
4ib4	--------GIE------TN-----PNNITCVLTK-------ERFGDFMLFGSLAAFFTPLAI
4iar	--RQA----------------------SECVVNT--------DHILYTVYSTVGAFYFPTLL

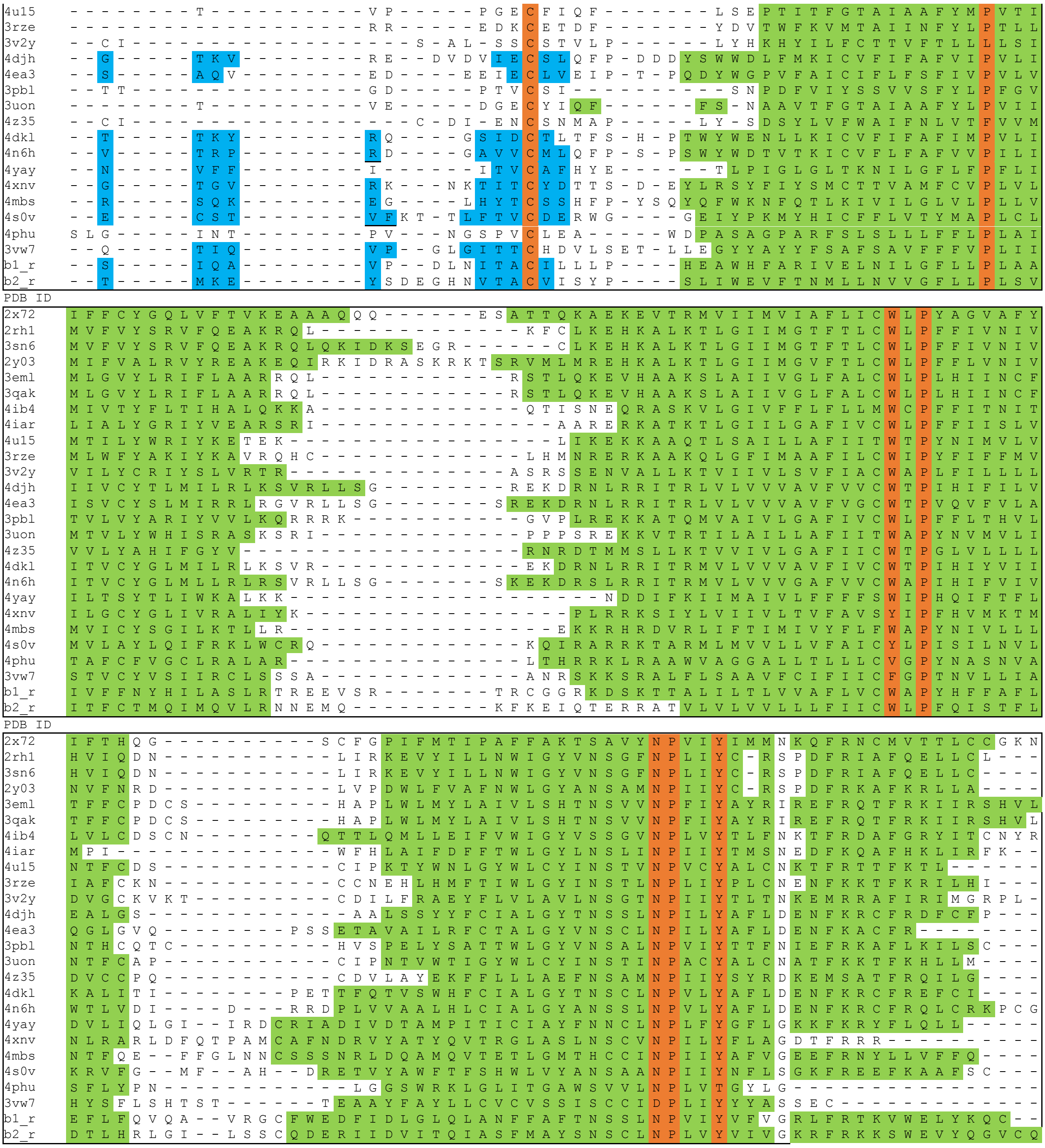

```
4u15   - - - - - - - - T - - - - - - - - - - - V P - - - - - P G E C F I Q F - - - - - - - L S E P T I T F G T A I A A F Y M P V T I
3rze   - - - - - - - - - - - - - - - - - - - R R - - - - - E D K C E T D F - - - - - - - Y D V T W F K V M T A I I N F Y L P T L L
3v2y   - - C I - - - - - - - - - - - - - - - - - - S - A L - S S C S T V L P - - - - - - L Y H K H Y I L F C T T V F T L L L L S I
4djh   - - G - - - - - T K V - - - - - - - - R E - - D V D V I E C S L Q F P - D D D Y S W W D L F M K I C V F I F A F V I P V L I
4ea3   - - S - - - - - A Q V - - - - - - - - E D - - - - E E I E C L V E I P - T - P Q D Y W G P V F A I C I F L F S F I V P V L V
3pbl   - - T T - - - - - - - - - - - - - - - G D - - - - - P T V C S I - - - - - - - - - - S N P D F V I Y S S V V S F Y L P F G V
3uon   - - - - - - - - T - - - - - - - - - - V E - - - - - D G E C Y I Q F - - - - - - F S - N A A V T F G T A I A A F Y L P V I I
4z35   - - C I - - - - - - - - - - - - - - - - - - C - D I - E N C S N M A P - - - - - L Y - S D S Y L V F W A I F N L V T F V V M
4dkl   - - T - - - - - T K Y - - - - - - - - R Q - - - - G S I D C T L T F S - H - P T W Y W E N L L K I C V F I F A F I M P V L I
4n6h   - - V - - - - - T R P - - - - - - - - R D - - - - G A V V C M L Q F P - S - P S W Y W D T V T K I C V F L F A F V V P I L I
4yay   - - N - - - - - V F F - - - - - - - - I - - - - - - I T V C A F H Y E - - - - - - T L P I G L G L T K N I L G F L F P F L I
4xnv   - - G - - - - - T G V - - - - - - - - R K - - - N K T I T C Y D T T S - D - E Y L R S Y F I Y S M C T T V A M F C V P L V L
4mbs   - - R - - - - - S Q K - - - - - - - - E G - - - - L H Y T C S S H F P - Y S Q Y Q F W K N F Q T L K I V I L G L V L P L L V
4s0v   - - E - - - - - C S T - - - - - - - - V F K T - T L F T V C D E R W G - - - - G E I Y P K M Y H I C F F L V T Y M A P L C L
4phu   S L G - - - - - I N T - - - - - - - - P V - - - N G S P V C L E A - - - - - W D P A S A G P A R F S L S L L L F F L P L A I
3vw7   - - Q - - - - - T I Q - - - - - - - - V P - - G L G I T T C H D V L S E T - L L E G Y Y A Y Y F S A F S A V F F F V P L I I
b1_r   - - S - - - - - I Q A - - - - - - - - V P - - D L N I T A C I L L L P - - - - H E A W H F A R I V E L N I L G F L L P L A A
b2_r   - - T - - - - - M K E - - - - - - - - Y S D E G H N V T A C V I S Y P - - - - S L I W E V F T N M L L N V V G F L L P L S V
PDB ID
2x72   I F F C Y G Q L V F T V K E A A A Q Q Q - - - - - - E S A T T Q K A E K E V T R M V I I M V I A F L I C W L P Y A G V A F Y
2rh1   M V F V Y S R V F Q E A K R Q L - - - - - - - - - - - - - K F C L K E H K A L K T L G I I M G T F T L C W L P F F I V N I V
3sn6   M V F V Y S R V F Q E A K R Q L Q K I D K S E G R - - - - - - C L K E H K A L K T L G I I M G T F T L C W L P F F I V N I V
2y03   M I F V A L R V Y R E A K E Q I R K I D R A S K R K T S R V M L M R E H K A L K T L G I I M G V F T L C W L P F F L V N I V
3eml   M L G V Y L R I F L A A R R Q L - - - - - - - - - - - - R S T L Q K E V H A A K S L A I I V G L F A L C W L P L H I I N C F
3qak   M L G V Y L R I F L A A R R Q L - - - - - - - - - - - - R S T L Q K E V H A A K S L A I I V G L F A L C W L P L H I I N C F
4ib4   M I V T Y F L T I H A L Q K K A - - - - - - - - - - - - - Q T I S N E Q R A S K V L G I V F F L F L L M W C P F F I T N I T
4iar   L I A L Y G R I Y V E A R S R I - - - - - - - - - - - - - - - A A R E R K A T K T L G I I L G A F I V C W L P F F I I S L V
4u15   M T I L Y W R I Y K E T E K - - - - - - - - - - - - - - - - - L I K E K K A A Q T L S A I L L A F I I T W T P Y N I M V L V
3rze   M L W F Y A K I Y K A V R Q H C - - - - - - - - - - - - - L H M N R E R K A A K Q L G F I M A A F I L C W I P Y F I F F M V
3v2y   V I L Y C R I Y S L V R T R - - - - - - - - - - - - - - A S R S S E N V A L L K T V I I V L S V F I A C W A P L F I L L L L
4djh   I I V C Y T L M I L R L K S V R L L S G - - - - - - - - R E K D R N L R R I T R L V L V V V A V F V V C W T P I H I F I L V
4ea3   I S V C Y S L M I R R L R G V R L L S G - - - - - - - S R E K D R N L R R I T R L V L V V V A V F V G C W T P V Q V F V L A
3pbl   T V L V Y A R I Y V V L K Q R R R K - - - - - - - - - - - G V P L R E K K A T Q M V A I V L G A F I V C W L P F F L T H V L
3uon   M T V L Y W H I S R A S K S R I - - - - - - - - - - - - - P P P S R E K K V T R T I L A I L L A F I I T W A P Y N V M V L I
4z35   V V L Y A H I F G Y V - - - - - - - - - - - - - - - - - - R N R D T M M S L L K T V V I V L G A F I I C W T P G L V L L L
4dkl   I T V C Y G L M I L R L K S V R - - - - - - - - - - - - - E K D R N L R R I T R M V L V V V A V F I V C W T P I H I Y V I I
4n6h   I T V C Y G L M L L R L R S V R L L S G - - - - - - - S K E K D R S L R R I T R M V L V V V G A F V V C W A P I H I F V I V
4yay   I L T S Y T L I W K A L K K - - - - - - - - - - - - - - - - - - - - N D D I F K I I M A I V L F F F F S W I P H Q I F T F L
4xnv   I L G C Y G L I V R A L I Y K - - - - - - - - - - - - - - - - - P L R R K S I Y L V I I V L T V F A V S Y I P F H V M K T M
4mbs   M V I C Y S G I L K T L L R - - - - - - - - - - - - - - - - - E K K R H R D V R L I F T I M I V Y F L F W A P Y N I V L L L
4s0v   M V L A Y L Q I F R K L W C R Q - - - - - - - - - - - - - K Q I R A R R K T A R M L M V V L L V F A I C Y L P I S I L N V L
4phu   T A F C F V G C L R A L A R - - - - - - - - - - - - - - - L T H R R K L R A A W V A G G A L L T L L L C V G P Y N A S N V A
3vw7   S T V C Y V S I I R C L S S S A - - - - - - - - - - - - - A N R S K K S R A L F L S A A V F C I F I I C F G P T N V L L I A
b1_r   I V F F N Y H I L A S L R T R E E V S R - - - - - - - T R C G G R K D S K T T A L I L T L V V A F L V C W A P Y H F F A F L
b2_r   I T F C T M Q I M Q V L R N N E M Q - - - - - - - - - K F K E I Q T E R R A T V L V L V V L L L F I I C W L P F Q I S T F L
PDB ID
2x72   I F T H Q G - - - - - - - - - - S C F G P I F M T I P A F F A K T S A V Y N P V I Y I M M N K Q F R N C M V T T L C C G K N
2rh1   H V I Q D N - - - - - - - - - - - L I R K E V Y I L L N W I G Y V N S G F N P L I Y C - R S P D F R I A F Q E L L C L - - -
3sn6   H V I Q D N - - - - - - - - - - - L I R K E V Y I L L N W I G Y V N S G F N P L I Y C - R S P D F R I A F Q E L L C - - - -
2y03   N V F N R D - - - - - - - - - - - L V P D W L F V A F N W L G Y A N S A M N P I I Y C - R S P D F R K A F K R L L A - - - -
3eml   T F F C P D C S - - - - - - - - - H A P L W L M Y L A I V L S H T N S V V N P F I Y A Y R I R E F R Q T F R K I I R S H V L
3qak   T F F C P D C S - - - - - - - - - H A P L W L M Y L A I V L S H T N S V V N P F I Y A Y R I R E F R Q T F R K I I R S H V L
4ib4   L V L C D S C N - - - - - - - - Q T T L Q M L L E I F V W I G Y V S S G V N P L V Y T L F N K T F R D A F G R Y I T C N Y R
4iar   M P I - - - - - - - - - - - - - - W F H L A I F D F F T W L G Y L N S L I N P I I Y T M S N E D F K Q A F H K L I R F K - -
4u15   N T F C D S - - - - - - - - - - - C I P K T Y W N L G Y W L C Y I N S T V N P V C Y A L C N K T F R T T F K T L - - - - - - -
3rze   I A F C K N - - - - - - - - - - - C C N E H L H M F T I W L G Y I N S T L N P L I Y P L C N E N F K K T F K R I L H I - - -
3v2y   D V G C K V K T - - - - - - - - - C D I L F R A E Y F L V L A V L N S G T N P I I Y T L T N K E M R R A F I R I M G R P L -
4djh   E A L G S - - - - - - - - - - - - - A A L S S Y Y F C I A L G Y T N S S L N P I L Y A F L D E N F K R C F R D F C F P - - -
4ea3   Q G L G V Q - - - - - - - - P S S E T A V A I L R F C T A L G Y V N S C L N P I L Y A F L D E N F K A C F R - - - - - - - -
3pbl   N T H C Q T C - - - - - - - - - - H V S P E L Y S A T T W L G Y V N S A L N P V I Y T T F N I E F R K A F L K I L S C - - -
3uon   N T F C A P - - - - - - - - - - - C I P N T V W T I G Y W L C Y I N S T I N P A C Y A L C N A T F K K T F K H L L M - - - -
4z35   D V C C P Q - - - - - - - - - - - C D V L A Y E K F F L L L A E F N S A M N P I I Y S Y R D K E M S A T F R Q I L G - - - -
4dkl   K A L I T I - - - - - - - - P E T T F Q T V S W H F C I A L G Y T N S C L N P V L Y A F L D E N F K R C F R E F C I - - - -
4n6h   W T L V D I - - - - D - - - R R D P L V V A A L H L C I A L G Y A N S S L N P V L Y A F L D E N F K R C F R Q L C R K P C G
4yay   D V L I Q L G I - - I R D C R I A D I V D T A M P I T I C I A Y F N N C L N P L F Y G F L G K K F K R Y F L Q L L - - - - - -
4xnv   N L R A R L D F Q T P A M C A F N D R V Y A T Y Q V T R G L A S L N S C V N P I L Y F L A G D T F R R R - - - - - - - - - -
4mbs   N T F Q E - - F F G L N N C S S S N R L D Q A M Q V T E T L G M T H C C I N P I I Y A F V G E E F R N Y L L V F F Q - - - -
4s0v   K R V F G - - M F - - A H - - D R E T V Y A W F T F S H W L V Y A N S A A N P I I Y N F L S G K F R E E F K A A F S C - - -
4phu   S F L Y P N - - - - - - - - - - - - L G G S W R K L G L I T G A W S V V L N P L V T G Y L G - - - - - - - - - - - - - - - -
3vw7   H Y S F L S H T S T - - - - - - T E A A Y F A Y L L C V C V S S I S C C I D P L I Y Y Y A S S E C - - - - - - - - - - - - -
b1_r   E F L F Q V Q A - - V R G C F W E D F I D L G L Q L A N F F A F T N S S L N P V I Y V F V G R L F R T K V W E L Y K Q C - -
b2_r   D T L H R L G I - - L S S C Q D E R I I D V I T Q I A S F M A Y S N S C L N P L V Y V I V G K R F R K K S W E V Y Q G V C Q
```

Supplementary Table 11: Comparison of peptide N-terminal binding region of B$_1$R from different mammals. The conserved binding residues are highlighted in yellow. The positions at which where changes in charge occur are labeled in red. Residue and BW numbering are based on human B$_1$R. All the non-rodent sequences as well as the common rat, mouse and Chinese hamster sequences were obtained from Uniprot. Sequences of other rodents were fished using Blast. The alignment were performed by Multalin server[25] using default parameters and the figure was prepared from the output of ESPript 3 (http://nar.oxfordjournals.org/content/42/W1/W320.long).

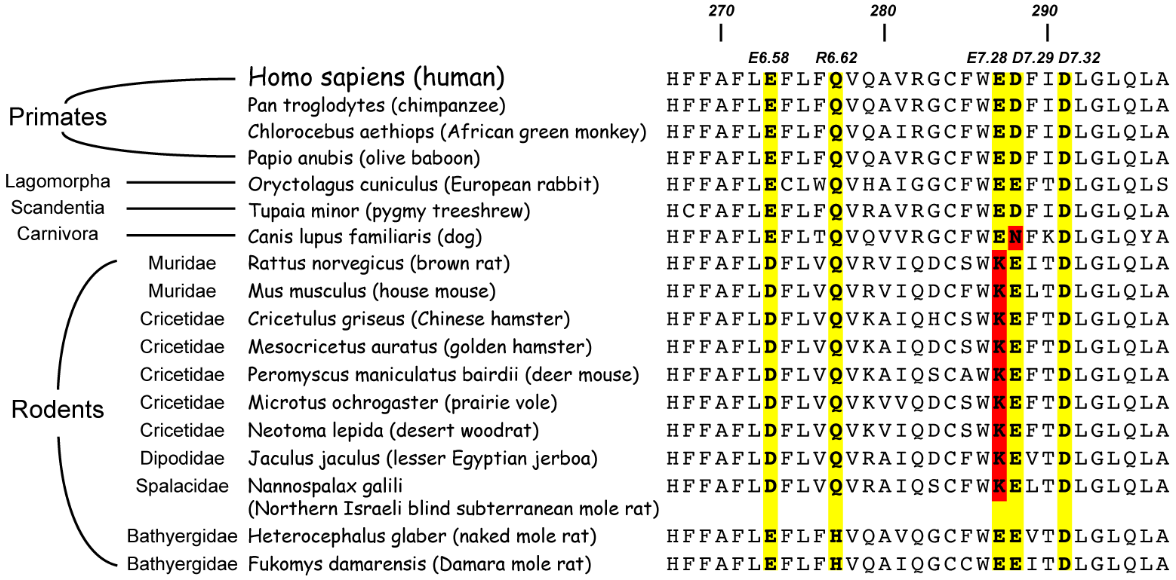

Primates		Homo sapiens (human)	HFFAFLEFLFQVQAVRGCFWEDFIDLGLQLA
		Pan troglodytes (chimpanzee)	HFFAFLEFLFQVQAVRGCFWEDFIDLGLQLA
		Chlorocebus aethiops (African green monkey)	HFFAFLEFLFQVQAIRGCFWEDFIDLGLQLA
		Papio anubis (olive baboon)	HFFAFLEFLFQVQAVRGCFWEDFIDLGLQLA
Lagomorpha		Oryctolagus cuniculus (European rabbit)	HFFAFLECLWQVHAIGGCFWEEFTDLGLQLS
Scandentia		Tupaia minor (pygmy treeshrew)	HCFAFLEFLFQVRAVRGCFWEDFIDLGLQLA
Carnivora		Canis lupus familiaris (dog)	HFFAFLEFLTQVQVVRGCFWENFKDLGLQYA
Rodents	Muridae	Rattus norvegicus (brown rat)	HFFAFLDFLVQVRVIQDCSWKEITDLGLQLA
	Muridae	Mus musculus (house mouse)	HFFAFLDFLVQVRVIQDCFWKELTDLGLQLA
	Cricetidae	Cricetulus griseus (Chinese hamster)	HFFAFLDFLVQVKAIQHCSWKEFTDLGLQLA
	Cricetidae	Mesocricetus auratus (golden hamster)	HFFAFLDFLVQVKAIQDCSWKEFTDLGLQLA
	Cricetidae	Peromyscus maniculatus bairdii (deer mouse)	HFFAFLDFLVQVKAIQSCAWKEFTDLGLQLA
	Cricetidae	Microtus ochrogaster (prairie vole)	HFFAFLDFLVQVKVVQDCSWKEFTDLGLQLA
	Cricetidae	Neotoma lepida (desert woodrat)	HFFAFLDFLVQVKVIQDCSWKEFTDLGLQLA
	Dipodidae	Jaculus jaculus (lesser Egyptian jerboa)	HFFAFLDFLVQVRAIQDCFWKEVTDLGLQLA
	Spalacidae	Nannospalax galili (Northern Israeli blind subterranean mole rat)	HFFAFLDFLVQVRAIQSCFWKELTDLGLQLA
	Bathyergidae	Heterocephalus glaber (naked mole rat)	HFFAFLEFLFHVQAVQGCFWEEVTDLGLQLA
	Bathyergidae	Fukomys damarensis (Damara mole rat)	HFFAFLEFLFHVQAIQGCCWEEITDLGLQLA

2. Supplementary Figures

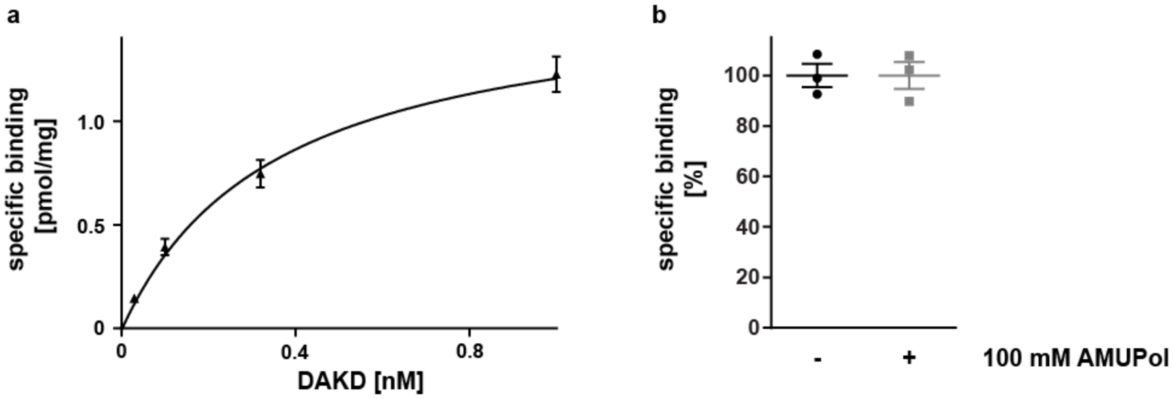

Supplementary Figure 1: DAKD binds with high affinity to detergent-solubilized B_1R (a) and total DAKD binding is not affected by the presence of the bi-nitroxide radical AMUPol (b). (a) Binding of DAKD to the B_1R solubilized in a mixed micelle of DDM and CHS can be saturated and takes place with high affinity (0.35 ± 0.08 nM), indicating that the receptor remains functional after solubilization from the membrane. (b) Total binding of DAKD to B_1R is not influenced by the presence of AMUPol confirming that radical addition does not disrupt the receptor-ligand complex before freezing the sample in the spectrometer. For both assays, B_1R was solubilized for 3 h in 1% DDM, 0.1% CHS in 50 mM HEPES-NaOH pH 7.6, 150 mM NaCl, 5% glycerol. Non-solubilized material was pelleted by ultracentrifugation. The receptor was immobilized on StrepTactin (StrepTactin SuperFlow Plus, Qiagen) beads and incubated with increasing concentrations of radiolabeled DAKD (Perkin Elmer) to determine the dissociation constant or with 10 nM radiolabeled DAKD in the presence of 100 mM AMUPol to assess the influence of the radical on total binding. Non-specific binding was assessed in the presence of 10 µM unlabeled DAKD. Bound from unbound ligand was separated by transferring StrepTactin-immobilized receptors onto GF/B filters and washing with 50 mM HEPES-NaOH pH 7.6, 150 mM NaCl, 5% glycerol, 0.05% DDM, 0.005% CHS. Remaining radioactivity was measured by liquid scintillation counting. The binding assays were carried out in triplicate (n=3).

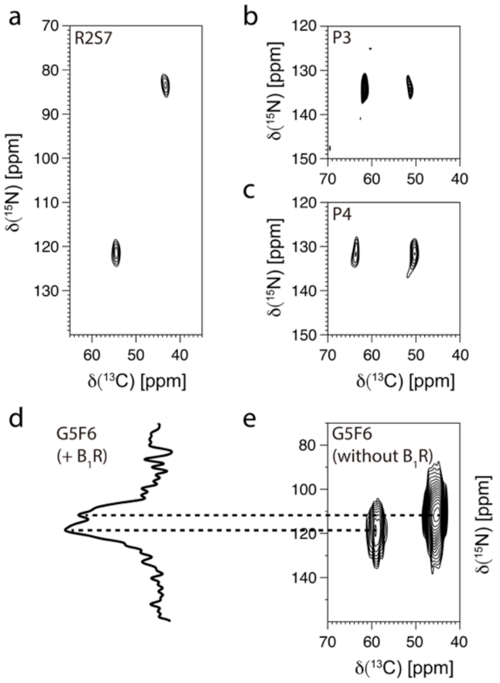

Supplementary Figure 2: Subsections of ^{15}N-^{13}C TEDOR spectra of differently labeled DAKD bound to B$_1$R. (a) U-[^{13}C,^{15}N]-R$_2$S$_7$ DAKD, (b) U-[^{13}C,^{15}N]-P$_3$ DAKD, (c) U-[^{13}C,^{15}N]-P$_4$ DAKD. Further subsections of U-[^{13}C,^{15}N]-R$_2$S$_7$ DAKD are shown in Supplementary Figure 7. Panel (d) presents CAN 1D ^{15}N spectra of U-[^{13}C,^{15}N]-G$_5$F$_6$ DAKD bound to B$_1$R. Panel (e) shows NCA spectra of this peptide without receptor. The ^{15}N chemical shifts of G5 and F6 can be easily assigned based on their characteristic values and high similarity to the values as indicated by the dashed horizontal lines.

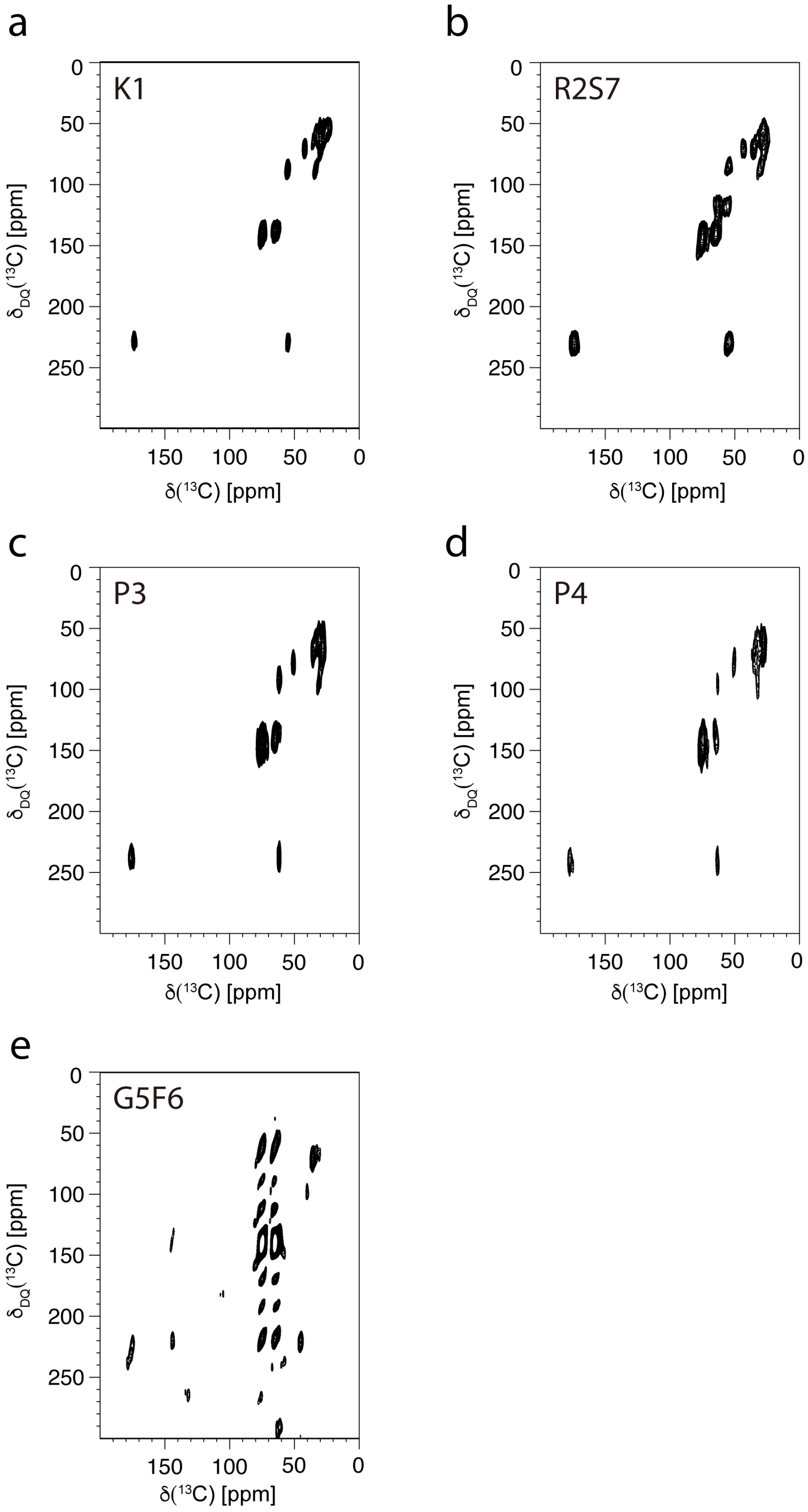

Supplementary Figure 3: DQ-SQ ^{13}C-^{13}C 2D spectra of DAKD bound to B$_1$R. (a) U-[^{13}C,^{15}N]-K$_1$ DAKD, (b) U-[^{13}C,^{15}N]-R$_2$S$_7$ DAKD, (c) U-[^{13}C,^{15}N]-P$_3$ DAKD, (d) U-[^{13}C,^{15}N]-P$_4$ DAKD, (e) U-[^{13}C,^{15}N]-G$_5$F$_6$ DAKD. The “ridge” in spectrum (e) is caused by the natural abundance ^{13}C-^{13}C pair in glycerol, which was significantly reduced by the use of ^{13}C-depleted glycerol in later measurements on other samples.

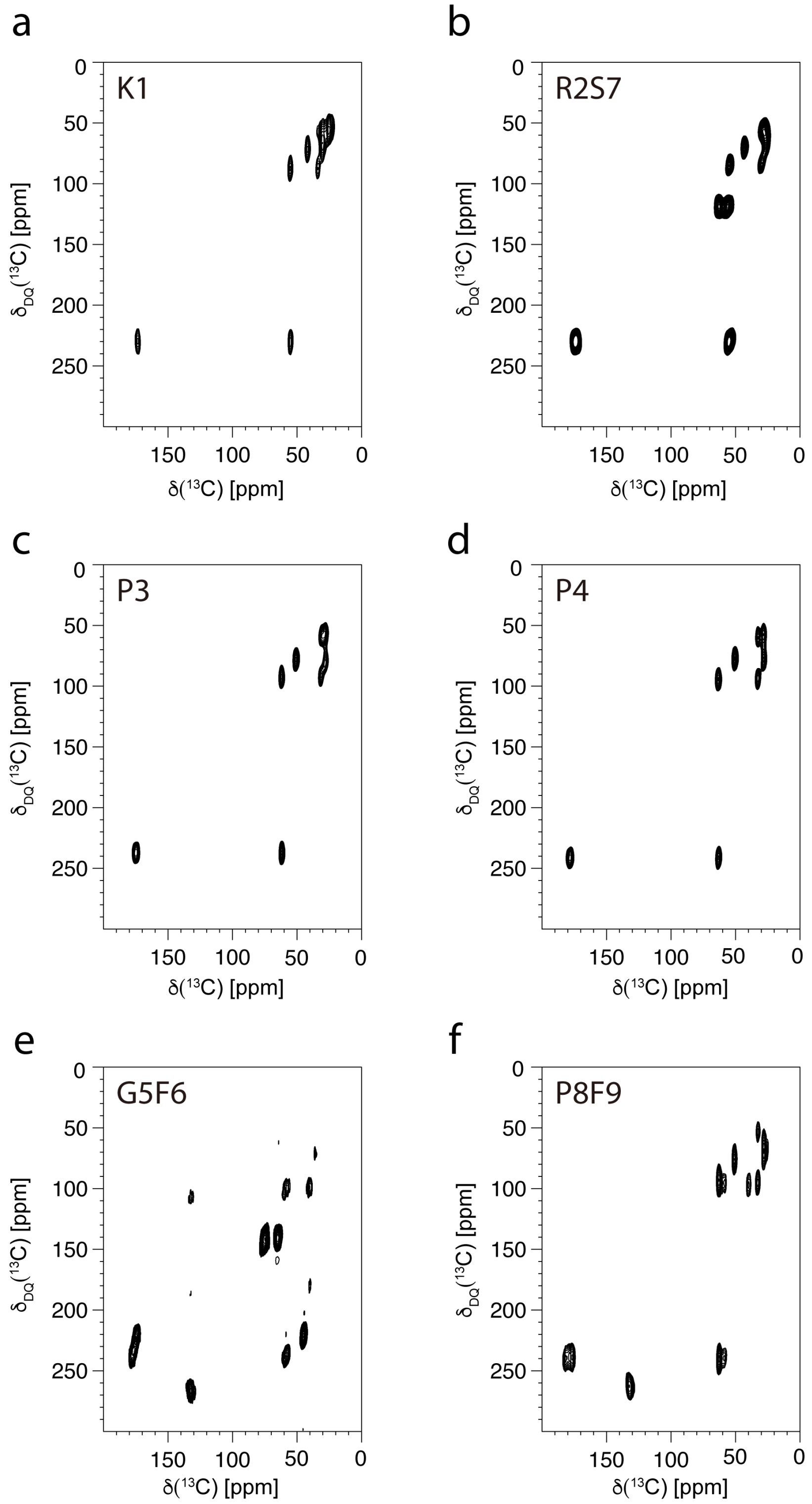

Supplementary Figure 4: DQ-SQ ^{13}C-^{13}C 2D spectra of DAKD without B$_1$R. (a) U-[^{13}C,^{15}N]-K$_1$ DAKD, (b) U-[^{13}C,^{15}N]-R$_2$S$_7$ DAKD, (c) U-[^{13}C,^{15}N]-P$_3$ DAKD, (d) U-[^{13}C,^{15}N]-P$_4$ DAKD, (e) U-[^{13}C,^{15}N]-G$_5$F$_6$ DAKD, (f) U-[^{13}C,^{15}N]-P$_8$F$_9$ DAKD.

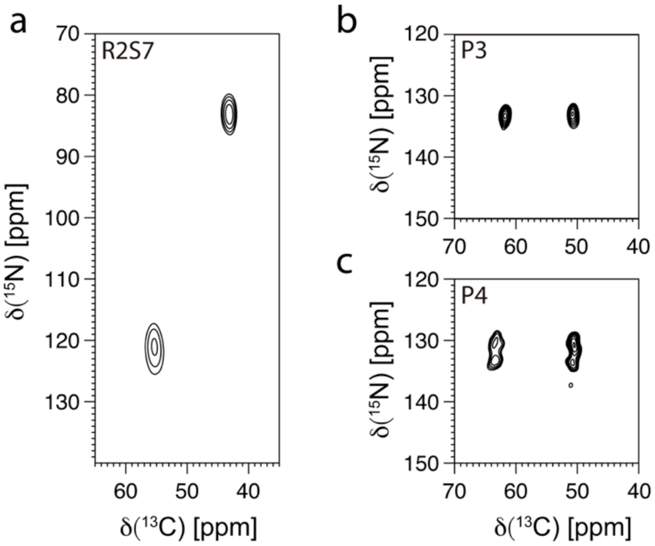

Supplementary Figure 5: ^{15}N-^{13}C 2D TEDOR spectra of DAKD peptide without receptor. The peptides were labeled using different labeling schemes (Supplementary Table 1). (a) U-[^{13}C,^{15}N]-R_2S_7 DAKD, (b) U-[^{13}C,^{15}N]-P_3 DAKD, (d) U-[^{13}C,^{15}N]-P_4 DAKD.

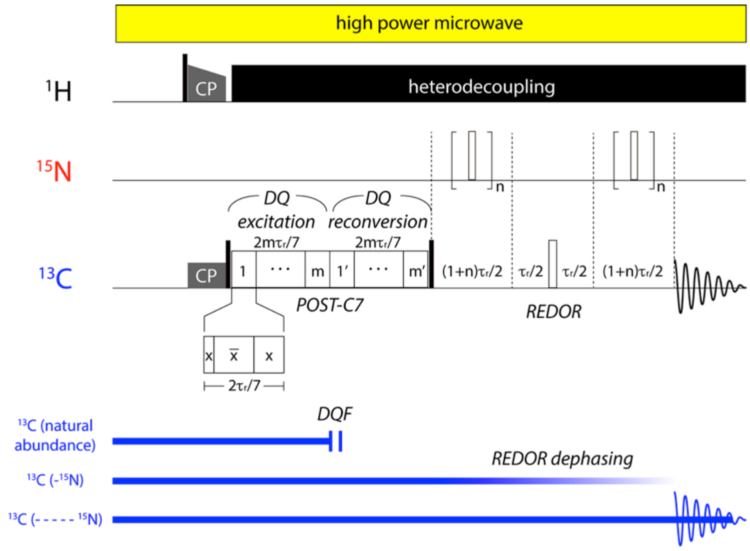

Supplementary Figure 6: DQ and REDOR doubly-filtered ^{13}C 1D pulse sequence used for acquiring the spectrum in Fig. 2f. The double-quantum-filter (DQF) removes efficiently natural abundance ^{13}C signals. Subsequently, ^{13}C magnetization of spins experiencing large ^{13}C-^{15}N dipolar couplings (e.g. from ^{13}C-^{15}N single bond distances) get dephased during a rotational-echo double-resonance spectroscopy (REDOR) recoupling period. The remaining signals mainly come from the ^{13}C labeled sites, which are further away from ^{15}N spins (i.e. those which are not directly bonded).

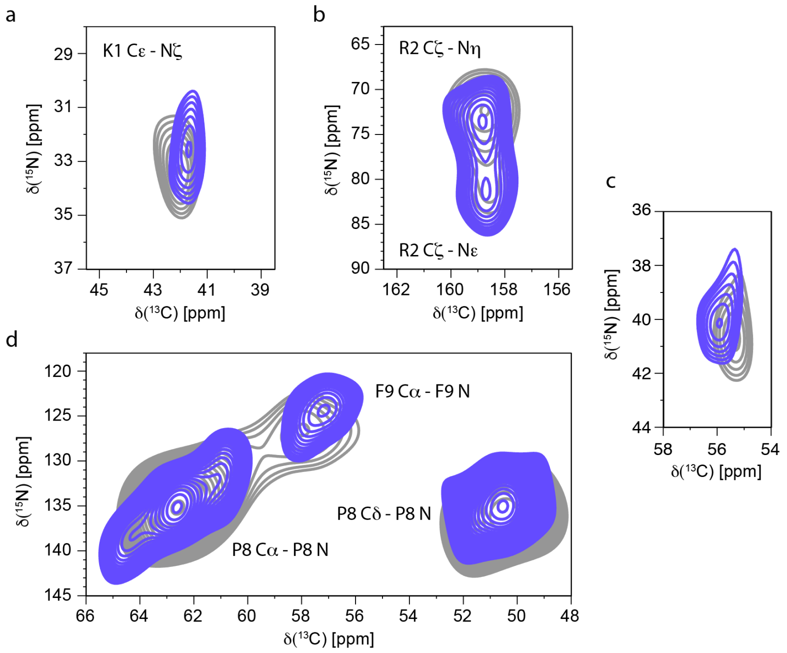

Supplementary Figure 7: Comparison of ^{15}N-^{13}C TEDOR 2D spectra of DAKD free (grey) and bound (blue) to B$_1$R. N- and C-terminal chemical shift changes: Lys and Arg side chain regions of ^{15}N-^{13}C TEDOR spectra of U-[^{13}C,^{15}N]-K$_1$ DAKD (a) and U-[^{13}C,^{15}N]-R$_2$S$_7$ DAKD (b). Chemical shift perturbations of the Cε-Nζ cross-peak of K1^{DAKD} and the Cζ-Nε cross-peak of R2^{DAKD} indicate the involvement of these side chains in binding. (c) Comparison of ^{15}N-^{13}C TEDOR 2D spectra of U-[^{13}C,^{15}N]-K$_1$ DAKD free and bound to B$_1$R. Small chemical shift changes on both the ^{13}C and ^{15}N dimensions are observed for amine ^{15}N /^{13}Cα cross peak of K1^{DAKD} upon binding to B$_1$R. (d) The ^{15}N-^{13}C TEDOR spectrum of U-[^{13}C,^{15}N]-P$_8$F$_9$ DAKD reveals a chemical shift change for the Cα-N cross-peak of F9^{DAKD} indicating a backbone conformational change upon binding.

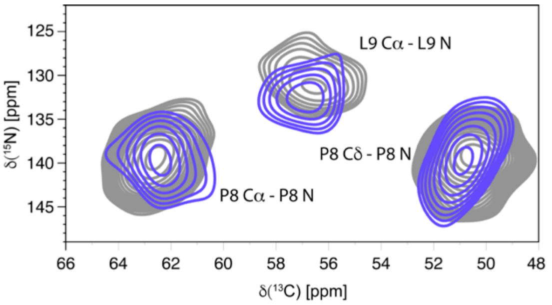

Supplementary Figure 8: ^{15}N-^{13}C TEDOR 2D spectra show significant backbone chemical shift changes of antagonist peptide U-[^{13}C,^{15}N]-P$_8$L$_9$ DALK upon binding to human B$_1$R. The spectrum of DALK bound to B$_1$R is shown in blue and the spectrum of DALK without receptor is shown in grey.

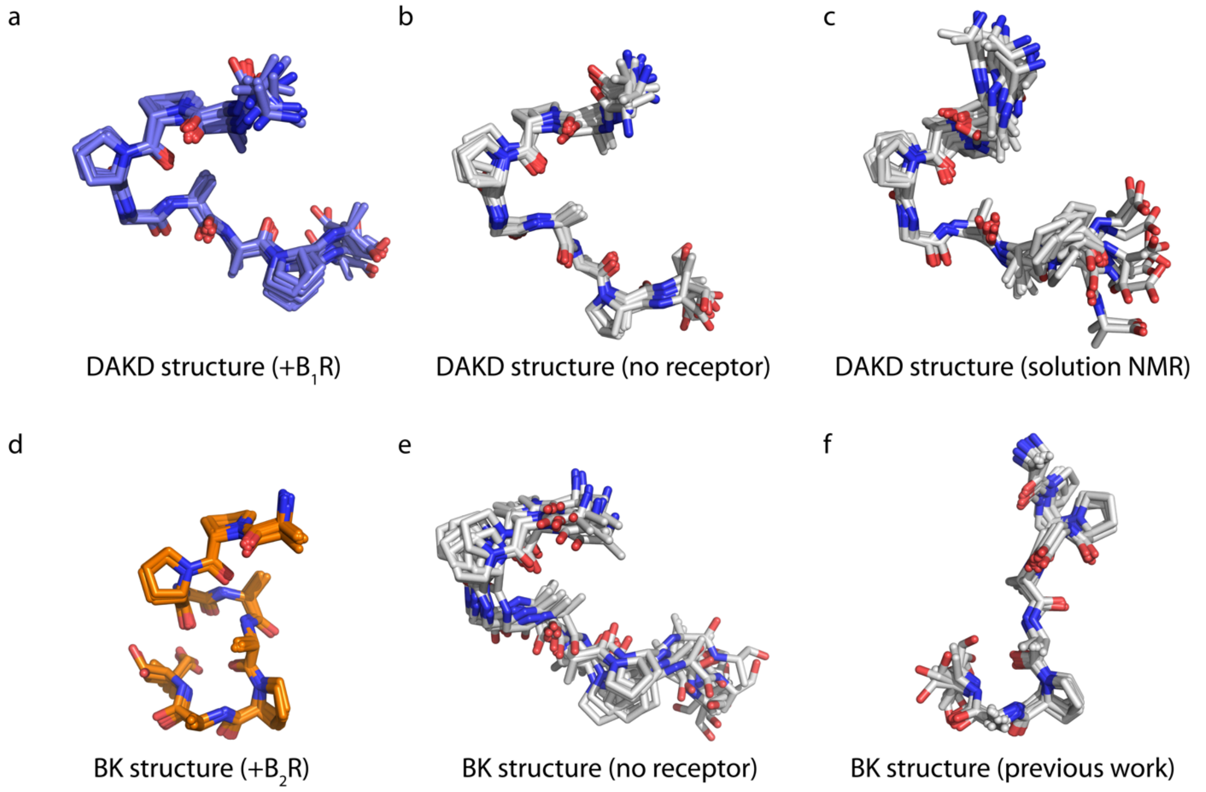

Supplementary Figure 9: Comparison of DAKD and BK NMR structures. DAKD bound to B_1R (a) and in frozen solution as determined from chemical shift by DNP-enhanced MAS-NMR (b). DAKD in solution determined by liquid-state NMR from chemical shifts and distance restraints (c). BK bound to B_2R re-calculated from TALOS+ from previously published chemical shifts[26] (d) and without receptor in frozen solution (e). Previously published structure of receptor-bound BK (f). Only backbone and Cβ atoms are shown. Each bundle contains 10 structures/models. The C-terminal residues of DAKD experience a subtle structural rearrangement upon binding to B_1R. In contrast, the C-terminal part of BK shows large conformational changes between receptor-bound and free states. The structure refinement statistics is summarized in Supplementary Tables 6-8.

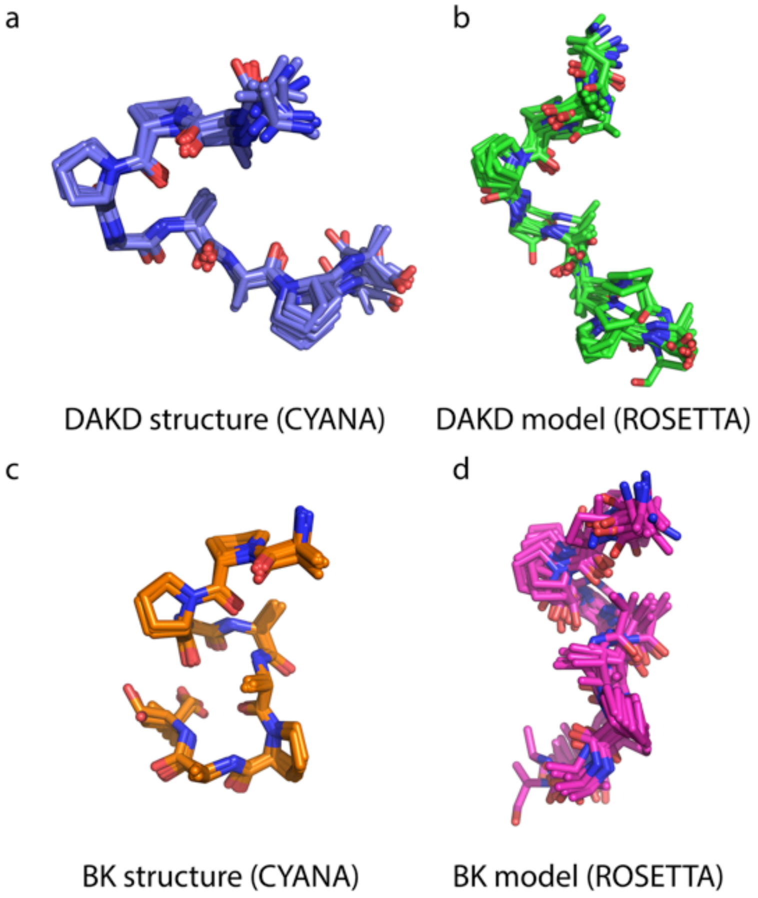

Supplementary Figure 10: Comparison of NMR structures (a,c) and Rosetta models (b,d) of DAKD (a,b) and BK (c,d) bound to human B_1R and human B_2R respective. Only backbone part and Cβ atoms of are shown. Each bundle contains 10 structures/models. The characteristic V-shape folding of DAKD (a) and S-shape folding of BK (c) were reproduced by Rosetta modeling (b,d). The backbone heavy atom RMSD between the final set of 10 Rosetta models and the NMR structure of BK is 2.1 Å on average. In case of DAKD, the average backbone RMSD between the Rosetta created ensemble and the NMR structural model obtained from the forward-predicted cluster A is 2.2 Å. The RMSD between the Rosetta created ensemble and the structure obtained by back-calculating from TALOS+ torsion angle restraints is 2.3 Å. Thus, the Rosetta models clearly confirm the overall structural motifs of both peptide ligands as inferred from the NMR chemical shift data. Some small torsion angle differences were observed between NMR and Rosetta models, which can be attributed to the receptor background in which the Rosetta modeling was performed. For DAKD, torsion angle differences for the first two N-terminal residues were observed, which could arise from some structural variability of ECL3 and thus different ligand interaction modes in our B_1R models. In case of BK, different values for the ϕ angle of $F8^{BK}$ and ψ angle of $P7^{BK}$ were obtained, reflecting a slightly more extended conformation of the C-terminal tail. Our B_2R binding model shows interactions of BK with TMH3 at the lower end of the binding pocket, which requires the C-terminus to stretch, leading to the described structural differences.

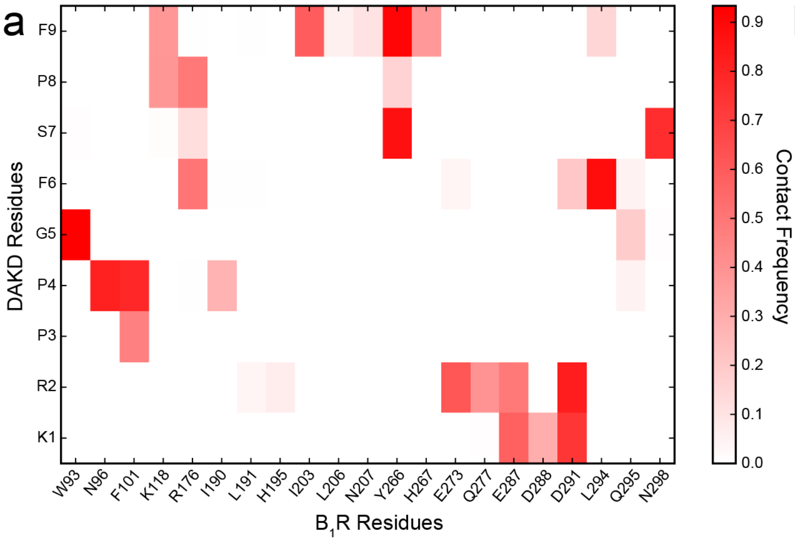

b

DAKD	B_1R	Freq. (%)	Score (REU)
G5	W93(2.60)	94	-2.30 +/- 0.44
F9	Y266(6.51)	92	-1.97 +/- 0.50
F6	L294(7.35)	89	-1.41 +/- 0.24
S7	W93(2.60)	88	-3.85 +/- 0.44
R2	D291(7.32)	83	-2.93 +/- 0.90
P4	N96(2.63)	82	-3.00 +/- 0.57
P4	F101(ECL1)	80	-1.44 +/- 0.20
S7	N298(7.39)	77	-3.87 +/- 1.51
K1	D291(7.32)	74	-1.89 +/- 0.22
R2	E273(6.58)	62	-3.66 +/- 0.94
F9	I203(5.39)	60	-1.44 +/- 0.33
K1	E287(7.28)	59	-1.79 +/- 0.36
F6	R176(ECL2)	51	-2.70 +/- 0.49
P8	R176(ECL2)	49	-1.25 +/- 0.22
R2	E287(7.28)	49	-2.33 +/- 1.09
P3	F101(ECL1)	47	-1.23 +/- 0.16
R2	Q277(6.62)	40	-2.72 +/- 0.56
P8	K118(3.33)	39	-2.52 +/- 0.86
F9	K118(3.33)	38	-2.24 +/- 0.92
F9	H267(6.52)	38	-1.73 +/- 0.51
K1	D288(7.29)	31	-1.66 +/- 0.42
P4	I190(ECL2)	28	-1.12 +/- 0.16
F6	D291(7.32)	21	-1.03 +/- 0.03
G5	Q295(7.36)	19	-1.89 +/- 0.29
P8	Y266(6.51)	16	-2.17 +/- 0.42

Supplementary Figure 11: Analysis of the B_1R-DAKD receptor-peptide interface. (a) Heatmap displaying the frequency of DAKD-B_1R contacts with a Rosetta score better than -1.0 REU as observed across the 1000 top docking models. (b) Summary of the 25 most frequent residue pairs in DAKD-B_1R models.

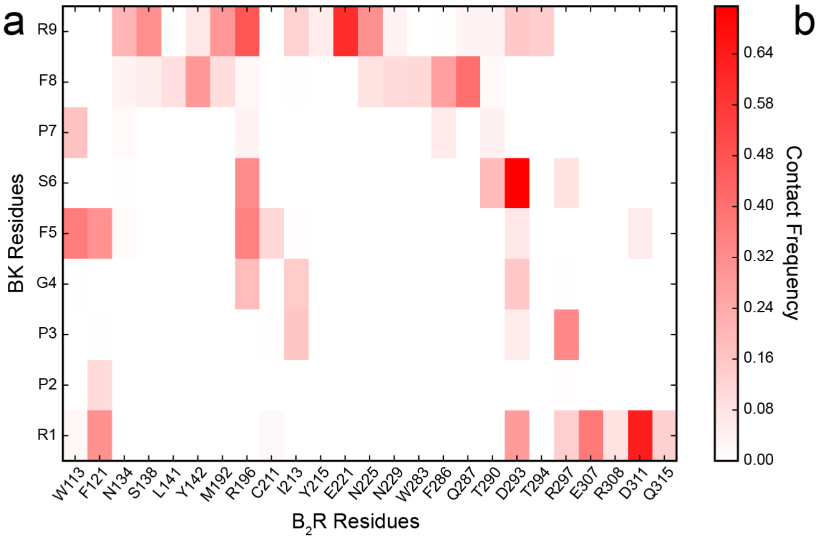

b

BK	B_2R	Freq. (%)	Score (REU)
S6	D293(6.58)	72	-2.76 +/- 0.89
R1	D311(7.32)	63	-2.81 +/- 1.13
R9	E221(5.35)	59	-3.12 +/- 1.29
R9	R196(ECL2)	47	-3.52 +/- 1.27
F8	Q287(6.52)	40	-1.60 +/- 0.74
R1	E307(7.28)	37	-2.58 +/- 1.10
F5	W113(2.60)	37	-1.74 +/- 0.67
F5	R196(ECL2)	35	-2.97 +/- 0.99
P3	R297(6.62)	33	-2.20 +/- 1.33
S6	R196(ECL2)	32	-2.63 +/- 0.75
R9	S138(3.33)	32	-3.04 +/- 0.59
R9	N225(5.39)	31	-1.89 +/- 0.83
R1	F121(ECL1)	31	-1.65 +/- 0.43
F5	F121(ECL1)	31	-1.42 +/- 0.36
R9	M192(4.60)	29	-1.28 +/- 0.23
F8	Y142(3.37)	29	-1.72 +/- 0.81
R1	D293(6.58)	28	-2.65 +/- 1.31
F8	F286(6.51)	27	-1.45 +/- 0.33
R9	N134(3.29)	21	-1.71 +/- 1.06
S6	T290(6.55)	20	-3.46 +/- 0.45
G4	R196(ECL2)	19	-2.34 +/- 0.88
P7	W113(2.60)	17	-1.22 +/- 0.18
P3	I213(ECL2)	16	-1.62 +/- 0.34
G4	D293(6.58)	16	-2.93 +/- 0.71
R9	D293(6.58)	15	-2.58 +/- 1.07

Supplementary Figure 12: Analysis of the B_2R-BK receptor-peptide interface. (a) Heatmap displaying the frequency of BK-B_2R contacts with a Rosetta score better than -1.0 REU as observed across the 1000 top docking models. (b) Summary of the 25 most frequent residue pairs in BK-B_2R models. The N-terminal residue $R1^{BK}$ is close to $D293^{6.58}$, $E307^{7.28}$ and $D311^{7.32}$ (Figures 5b,d). Its positively charged amine-terminus and side chain make multiple interactions with these residues. We found the $R1^{BK}$ side chain not in a single position but instead to sample several orientations and make electrostatic interactions with $D293^{6.58}$ and $D311^{7.32}$ as well as H-bond contacts with $Q315^{7.36}$. At its C-terminal end, BK is fixed by an H-bond between the $R9^{BK}$ carboxyl group and residue $S138^{3.33}$, which is structurally similar to the DAKD-B_1R complex where $F9^{DAKD}$ interacts with $K118^{3.33}$ (Figures 5b,f). The side chain of $R9^{BK}$ was found to participate in frequent interactions with $E221^{5.35}$ and $N225^{5.39}$ at the extracellular end of TMH V (Figure 5f). The BK C-terminus is further stabilized by B_2R residue $F286^{6.51}$, which has a strong effect on ligand binding[27]. We observed this residue to pack against $P7^{BK}$ and $F8^{BK}$ and, together with $L141^{3.36}$, $Y142^{3.37}$ and $T290^{6.56}$, form a hydrophobic environment for $F8^{BK}$ (Figure 5f). A contribution of $Y142^{3.37}$ and $T290^{6.56}$ to ligand binding can be inferred from the available mutational data, too. Furthermore, our B_2R binding model predicts several interactions that have not been described before, such as hydrophobic contacts between $F5^{BK}$ and the aromatic side chains of $W113^{2.60}$ and F121 in ECL1 as well as several H-bonds between the central portion of the BK backbone and R196 in ECL2. Interestingly, we have identified and experimentally validated the corresponding residues in B_1R ($W93^{2.60}$, F101 and R176) as important DAKD interactions sites, which suggests that this group of conserved receptor residues is important for binding the middle region of both peptide ligands. For example, R176 in B_1R and R196 in B_2R, play a similar role as H-bond donor. However, due to its more extended, open conformation DAKD forms a dense H-bond network with R176 and additional receptor residues, which is not observed to this high extent for BK.

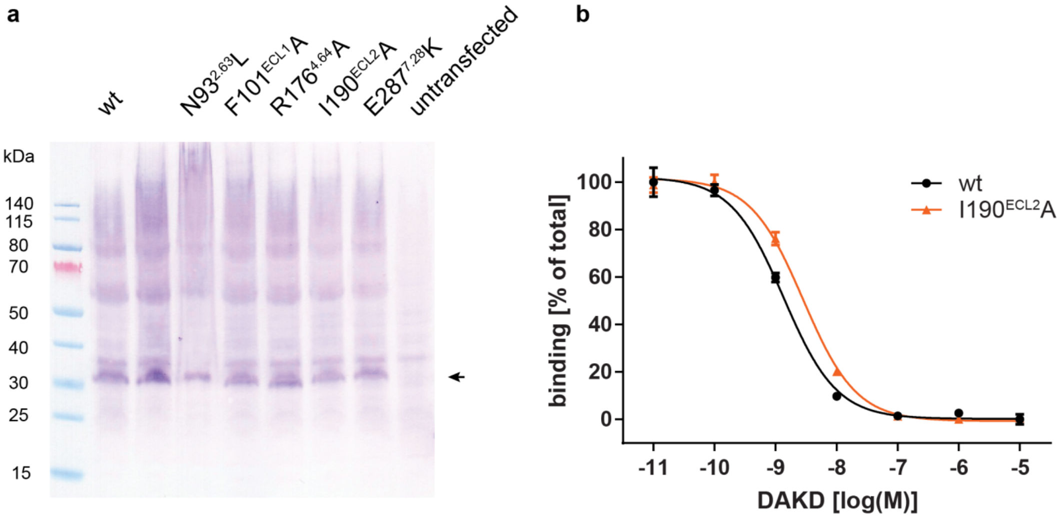

Supplementary Figure 13: Expression of B_1R mutants (a) and competition binding experiments of wild type and I190^{ECL2}A B_1R (b). The expression level of B1R mutants was assessed by Western blot using an M2 FLAG antibody against the N-terminal FLAG tag. All mutants express comparably to wild type (wt). The lane between wt and N93$^{2.63}$L contains an unrelated sample. (b) Competition binding analysis of wild type and I190ECL2A B1R expressed in HEK cells. Replacing I190$_{ECL2}$ with an alanine residue results in a slight decrease of the IC$_{50}$ of DAKD (I190$_{ECL2}$A 2.8 ± 0.2 nM, wild type (wt) 1.4 ± 0.7 nM; n=2). See Figure 4b for comparative binding experiments.

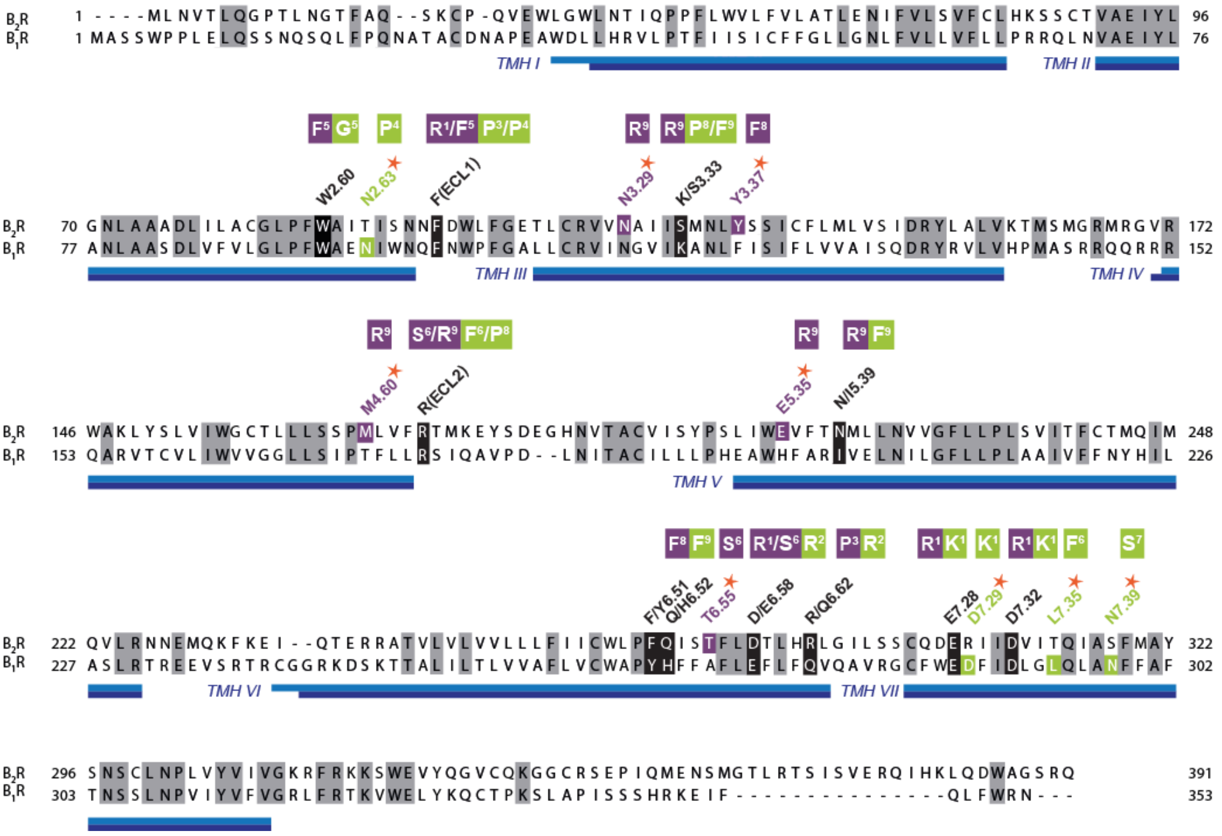

s

Supplementary Figure 14: Alignment of the amino acid sequences of the B_2R and B_1R highlighting residues interacting with the respective peptide ligands (purple for BK-B_2R and green for DAKD-B_1R interactions, respectively). Conserved residues in the receptor sequences interacting with residues of the peptide ligands are colored black, residues specifically interacting in only one of the receptors are colored purple (B_2R) or green (B_1R). The positions of the transmembrane helices (TMH) are shown as dark blue (B_2R) or light blue bars (B_1R) and correspond to the positions in the models used here. Residues specifically interacting with peptide ligands in only one of the kinin receptors are highlighted with stars. For clarity the sequence of isoform 2 (short isoform) of the B_2R was used in this alignment and annotated using the numbering of isoform 1 (long isoform).

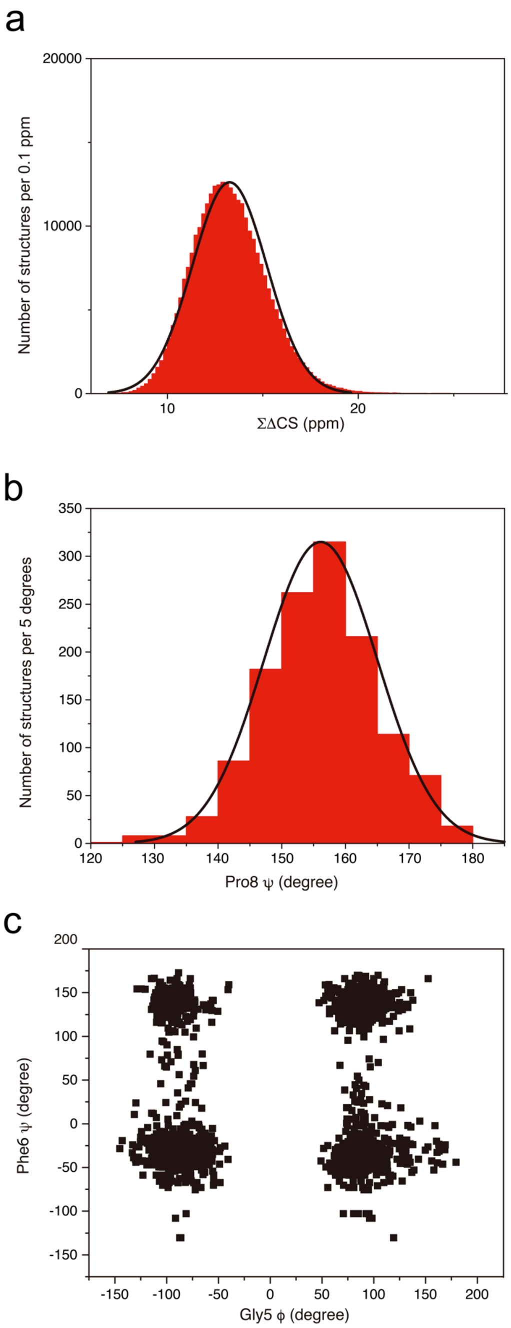

Supplementary Figure 15: Characteristics of Flexible-Meccano/SHIFTX-based forward chemical shift fitting approach on B_1R-bound DAKD. (a) Overall Gaussian-like distribution of conformations along ΣΔCS in Flexible-Meccano/SHIFTX approach. (b) An example showing the Gaussian-like torsion angle distribution in the top 1490 structures selected by the parameter *cutoff* (see online methods). (c) An example showing independent torsion angle ambiguity in torsion angle restraints obtained from top 1490 structures in the Flexible Meccano/SHIFTX-based forward fitting.

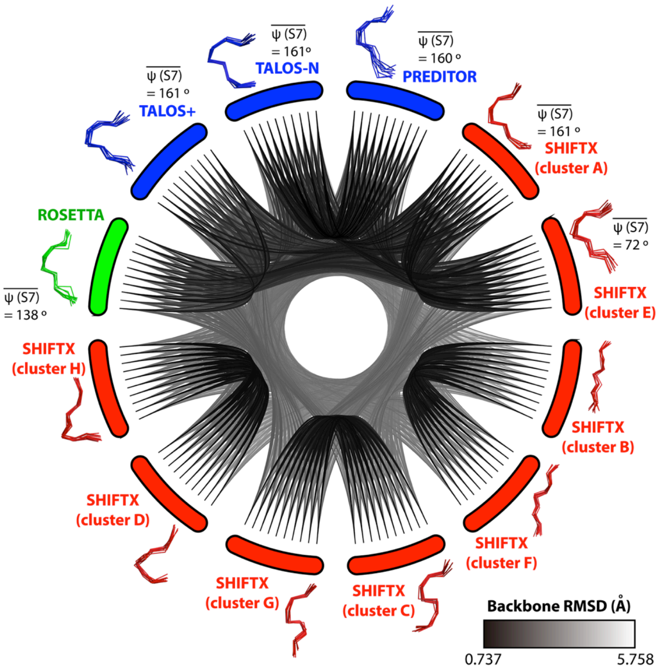

Supplementary Figure 16: RMSD analysis of DAKD structures/models generated using different approaches. The string plot is generated using CIRCOS-0.69.3[28].

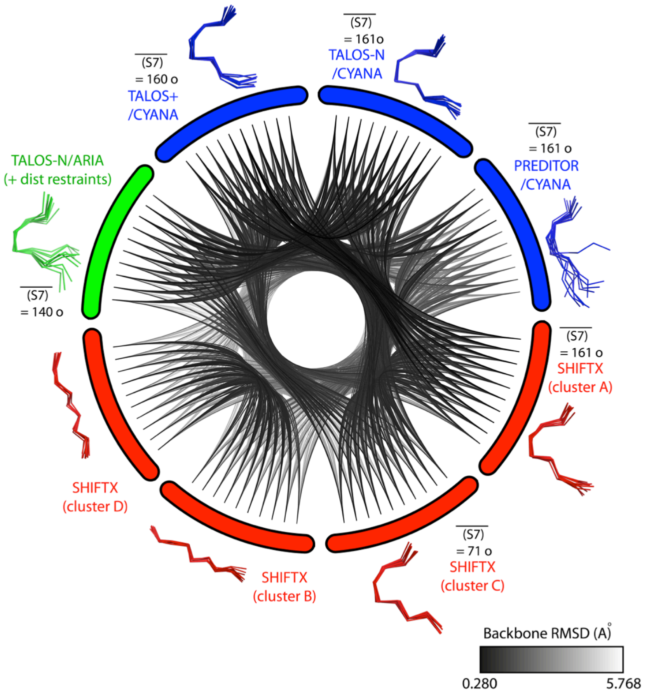

Supplementary Figure 17: RMSD analysis of non-bound DAKD structures/models generated using different approaches. The string plot is generated using CIRCOS-0.69.3[28].

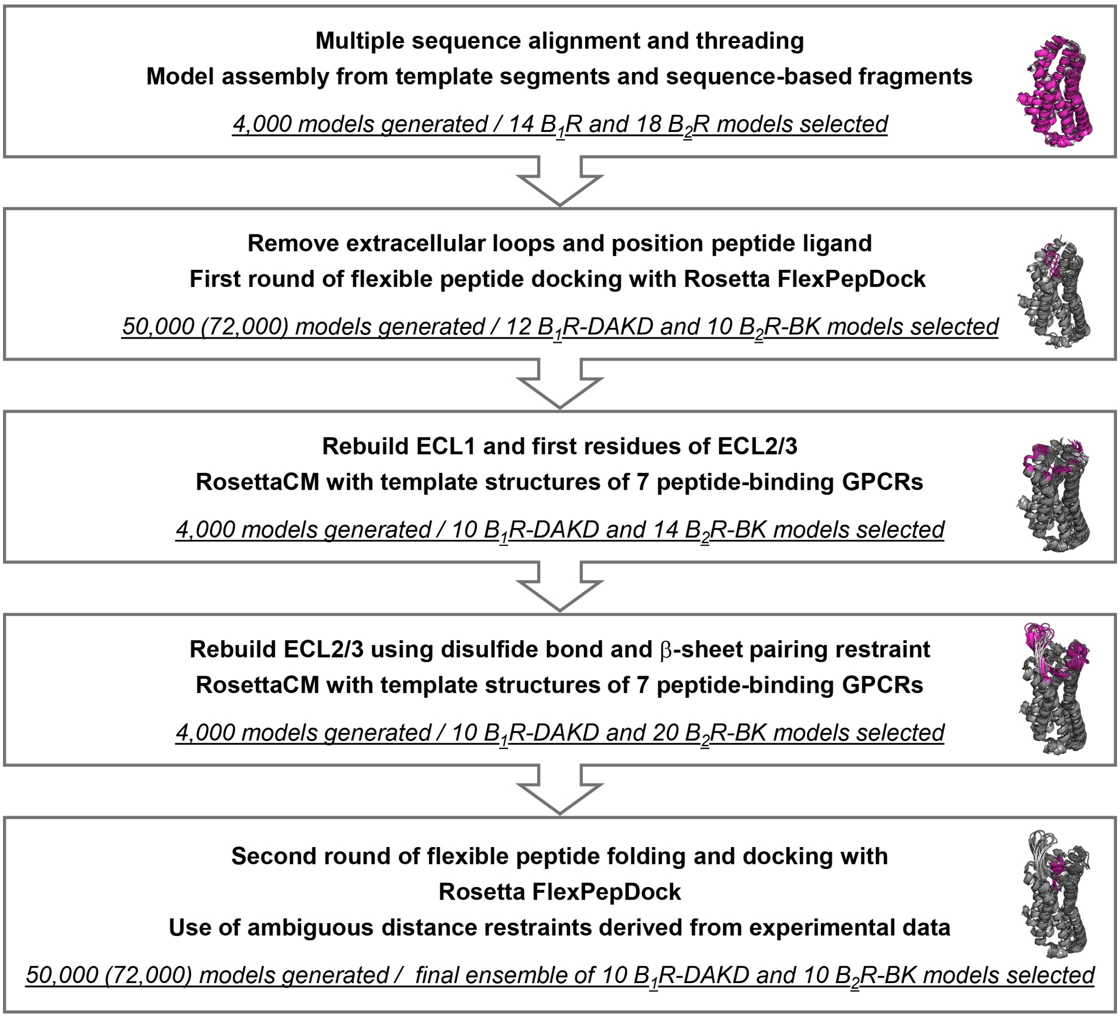

Supplementary Figure 18: Workflow of B_1R-DAKD and B_2R-bradykinin modeling and docking. Ensembles of B_1R and B_2R models in complex with their endogenous ligands DAKD and bradykinin were constructed by several rounds of comparative modeling, loop building and ligand docking. Comparative modeling of the transmembrane helix region was performed using 24 GPCR template structures, whereas for loop modeling only seven peptide-binding GPCRs with higher sequence similarity to B_1R and B_2R were used as templates. Peptide docking was guided by loose distance restraints derived from mutational data previously reported for B_1R and B_2R. Representative models for each modeling stage are depicted in the flowchart. For selecting the final cluster, a chemical shift filtering step was applied (see online methods).

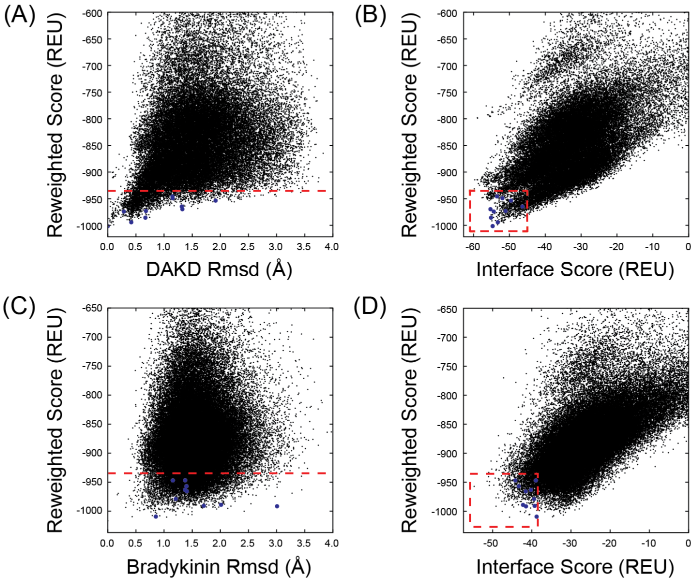

Supplementary Figure 19: Rosetta reweighted score vs. peptide backbone RMSD and interface score plots for docking of DAKD to B_1R (A and B) and bradykinin to B_2R (C and D). The ten largest clusters (shown as blue circles) were created from the best 1,000 models by reweighted and interface score (area within the red rectangle). The reweighted score combine the Rosetta total, peptide and interface energy.

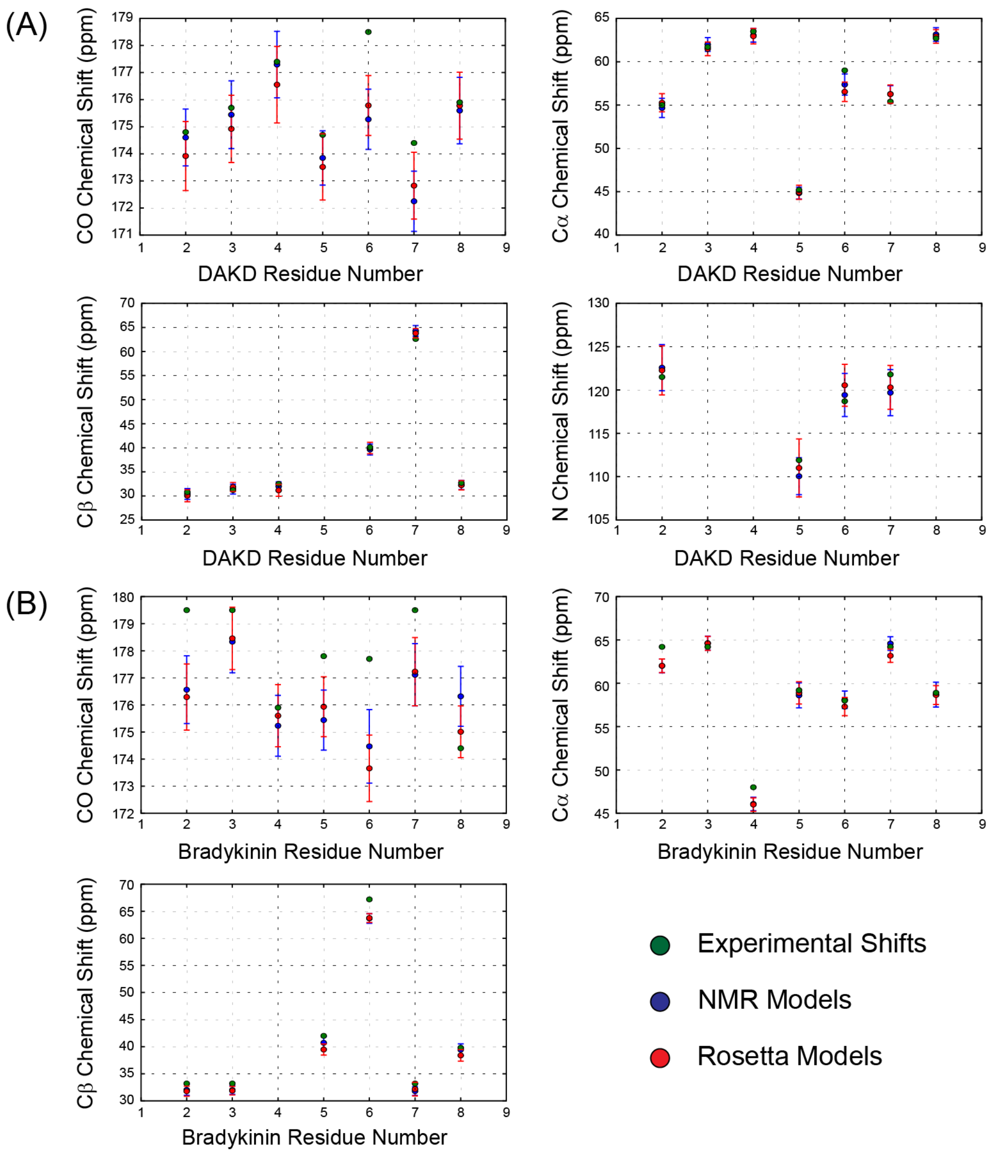

Supplementary Figure 20: Comparison of experimental and SPARTA+ back-calculated chemical shifts for NMR and Rosetta structural models of (A) DAKD and (B) bradykinin. Calculated chemical shifts represent the average of the final NMR structural models, as obtained by the forward prediction method (DAKD, cluster A) or by the TALOS+ method (BK) and the 10 final Rosetta models. Error bars depict the prediction uncertainty of SPARTA+. Chemical shift values of the first and last residue were not calculated because the prediction requires torsion angle information from two direct neighbor residues. The SPARTA+ calculated chemical shifts for the presented Rosetta ensemble of DAKD and BK gave an average RMSD of 1.33 ± 0.07 ppm and 1.99 ± 0.10 ppm, respectively, which compares to 1.34 ± 0.14 ppm and 1.82 ± 0.06 ppm for the respective NMR models. Using SHIFTX2, a comparable good agreement was obtained and RMSD values were 1.56 ± 0.10 ppm and 1.98 ± 0.06 ppm for Rosetta models and 1.65 ± 0.15 ppm and 1.89 ± 0.06 ppm for NMR models of DAKD and BK, respectively.

4. References

1. Zhang, H. et al. Structure of the Angiotensin receptor revealed by serial femtosecond crystallography. *Cell* **161**, 833-844 (2015).
2. Tan, Q. et al. Structure of the CCR5 chemokine receptor-HIV entry inhibitor maraviroc complex. *Science* **341**, 1387–1390 (2013).
3. Wu, H. et al. Structure of the human κ-opioid receptor in complex with JDTic. *Nature* **485**, 327–332 (2012).
4. Yin, J. et al. Structure and ligand-binding mechanism of the human OX1 and OX2 orexin receptors. *Nat. Struct. Mol. Biol.* **23**, 293-299 (2016).
5. Zhang, D. et al. Two disparate ligand-binding sites in the human P2Y1 receptor. *Nature* **520**, 317-321 (2015).
6. Fenalti, G. et al. Molecular control of δ-opioid receptor signalling. *Nature* **506**, 191–196 (2014).
7. Manglik, A. et al. Crystal structure of the μ-opioid receptor bound to a morphinan antagonist. *Nature* **485**, 321–326 (2012).
8. Chrencik, J.E. et al. Crystal Structure of Antagonist Bound Human Lysophosphatidic Acid Receptor 1. *Cell* **161**, 1633-1643 (2015).
9. Thompson, A.A. et al. Structure of the nociceptin/orphanin FQ receptor in complex with a peptide mimetic. *Nature* **485**, 395–399 (2012).
10. Standfuss, J. et al. The structural basis of agonist-induced activation in constitutively active rhodopsin. *Nature* **471**, 656–660 (2011).
11. Wacker, D. et al. Structural features for functional selectivity at serotonin receptors. *Science* **340**, 615–619 (2013).
12. Warne, T. et al. The structural basis for agonist and partial agonist action on a beta(1)-adrenergic receptor. *Nature* **469**, 241-244 (2011).
13. Zhang, C. et al. High-resolution crystal structure of human protease-activated receptor 1. *Nature* **492**, 387–392 (2012).
14. Haga, K. et al. Structure of the human M2 muscarinic acetylcholine receptor bound to an antagonist. *Nature* **482**, 547–551 (2012).
15. Shimamura, T. et al. Structure of the human histamine H1 receptor complex with doxepin. *Nature* **475**, 65–70 (2011).
16. Thorsen, T.S., Matt, R., Weis, W.I. & Kobilka, B.K. Modified T4 Lysozyme Fusion Proteins Facilitate G Protein-Coupled Receptor Crystallogenesis. *Structure* **22**, 1657-1664 (2014).
17. Rasmussen, S.G.F. et al. Crystal structure of the β2 adrenergic receptor-Gs protein complex. *Nature* **477**, 549–555 (2011).
18. Cherezov, V. et al. High-resolution crystal structure of an engineered human beta2-adrenergic G protein-coupled receptor. *Science* **318**, 1258-1265 (2007).
19. Xu, F. et al. Structure of an agonist-bound human A2A adenosine receptor. *Science* **332**, 322–327 (2011).
20. Jaakola, V.P. et al. The 2.6 angstrom crystal structure of a human A2A adenosine receptor bound to an antagonist. *Science* **322**, 1211-1217 (2008).
21. Hanson, M.A. et al. Crystal structure of a lipid G protein-coupled receptor. *Science* **335**, 851–855 (2012).
22. Chien, E.Y.T. et al. Structure of the human dopamine D3 receptor in complex with a D2/D3 selective antagonist. *Science* **330**, 1091–1095 (2010).
23. Wang, C. et al. Structural basis for molecular recognition at serotonin receptors. *Science* **340**, 610–614 (2013).
24. Srivastava, A. et al. High-resolution structure of the human GPR40 receptor bound to allosteric agonist TAK-875. *Nature* **513**, 124–127 (2014).
25. Corpet, F. Multiple sequence alignment with hierarchical-clustering. *Nucleic Acids Res.* **16**, 10881-10890 (1988).
26. Lopez, J.J. et al. The structure of the neuropeptide bradykinin bound to the human G-protein coupled receptor bradykinin B2 as determined by solid-state NMR spectroscopy. *Angew. Chem. Int. Ed.* **47**, 1668-1671 (2008).
27. Jarnagin, K. et al. Mutations in the B2 bradykinin receptor reveal a different pattern of contacts for peptidic agonists and peptidic antagonists. *J. Biol. Chem.* **271**, 28277–28286 (1996).
28. Krzywinski, M. et al. Circos: An information aesthetic for comparative genomics. *Genome Res.* **19**, 1639-1645 (2009).